Supplementary Material

Understanding the Influence of Stratification for Mine Water Management: A Comparative Study

Elke Mugova[1], **Christian Wolkersdorfer**[2]

[1]Technische Universität Bergakademie Freiberg (TUBAF), Department of Hydrogeology and Hydrochemistry, Otto-Meißer-Bau, Gustav-Zeuner-Str. 12, 09599 Freiberg, Germany, elke.mugova@grubenwasser.org, ORCID: 0000-0001-6019-9945

[2]South African Research Chair for Acid Mine Drainage Treatment, Tshwane University of Technology (TUT), Private Bag, X680, Pretoria, 0001, South Africa, christian@wolkersdorfer.info, ORCID: 0000-0003-2035-1863

Table of Content

Siège Merlebach (Vouters) colliery 3

Siège Merlebach (Simon 5) colliery 4

Kukla and Jindřich colliery 5

Hermann colliery 7

Velsen colliery 9

Glückaufsegen colliery........ 10

Friedlicher Nachbar colliery 11

San Vincente colliery 12

Horden colliery 14

Merkur lead mine 15

Straßberg fluorspar mine 16

Meggen mine........ 20

West Rand gold mine #8 Shaft 21

Leopold-Louise iron ore mine 22

Hancock copper mine 23

Georg iron ore mine 24

Stahlberg iron ore........ 25

Urgeiriça uranium mine........ 27

Metsämonttu mine 28

Aijala mine 30

Georgi Unterbau silver-copper mine........ 31

Groverake fluorspar mine 33

Roudný gold mine........ 35

Table: Observations about the topmost (first) intermediate........ 36

Glossary 39

References for Glossary........ 42

Siège Merlebach (Vouters) colliery

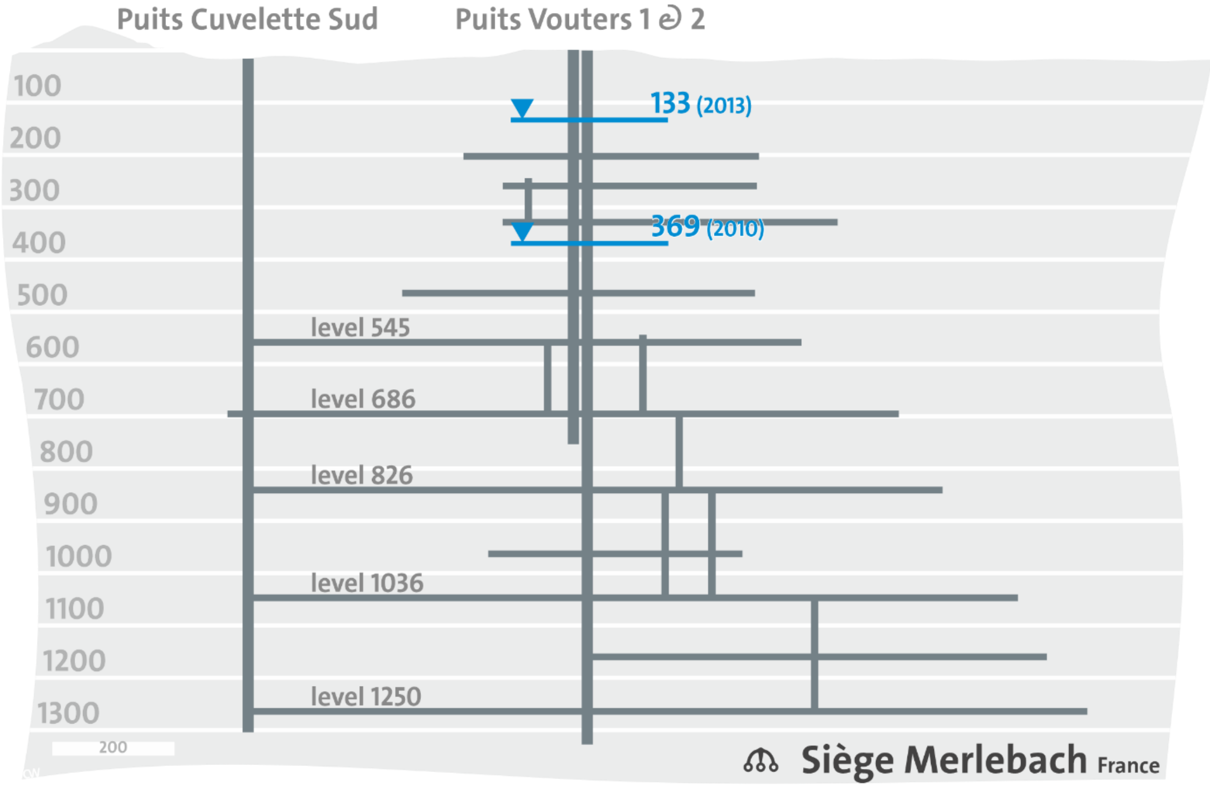

Figure S 1: Cross section of the Siège Merlebach (Vouters) colliery in France.

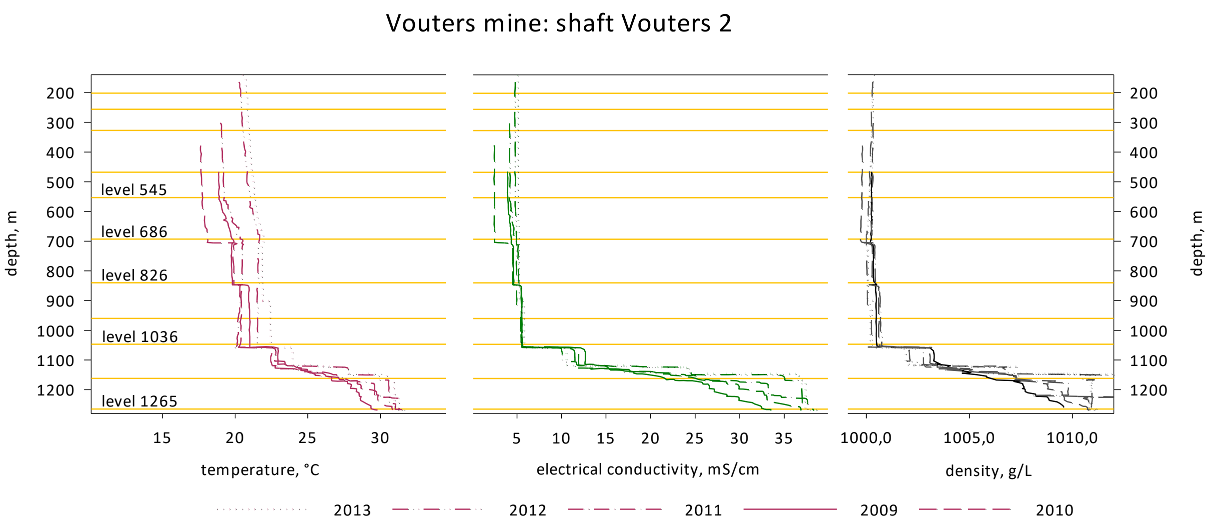

Figure S 2: Temperature profiles (measured), electrical conductivity profiles (measured) and density profiles (calculated with UNESCO equation) of the flooded Vouters 2 shaft at the Siège Merlebach (Vouters) colliery in France.

Siège Merlebach (Simon 5) colliery

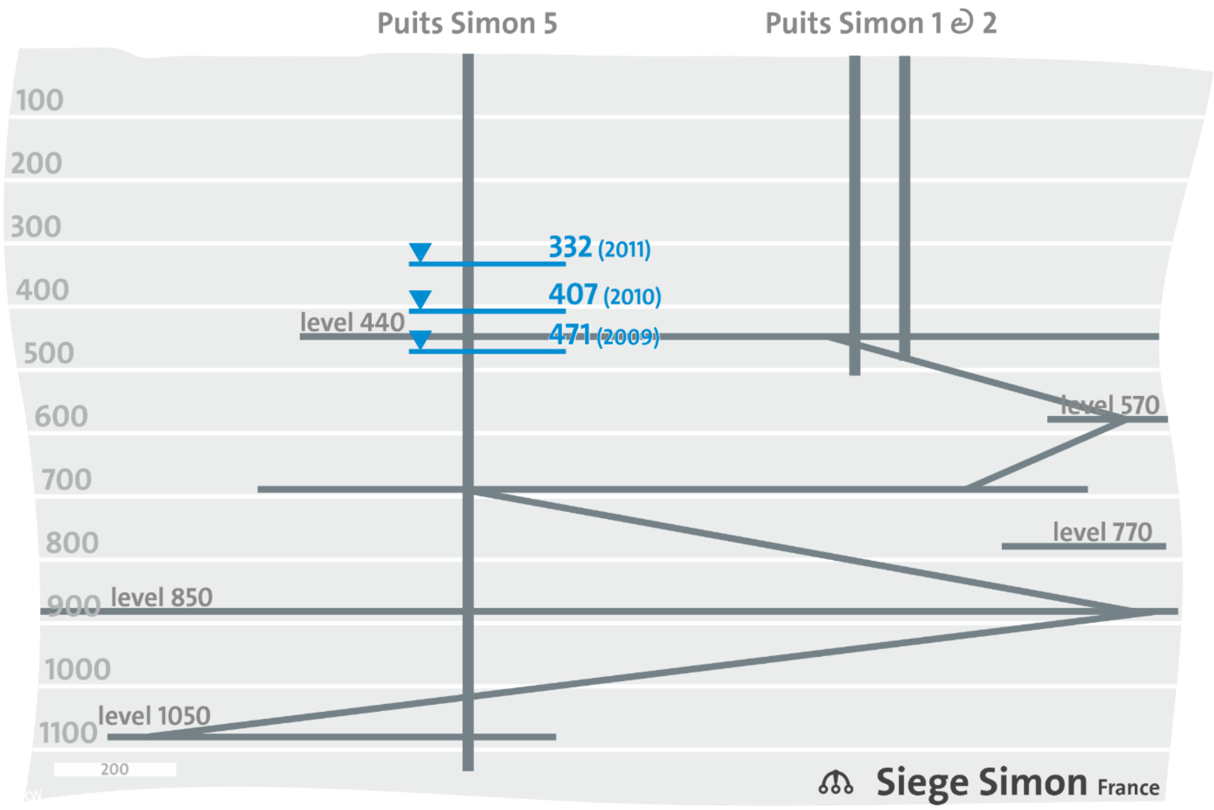

Figure S 3: Cross section of the Siège Merlebach (Simon 5) colliery in France.

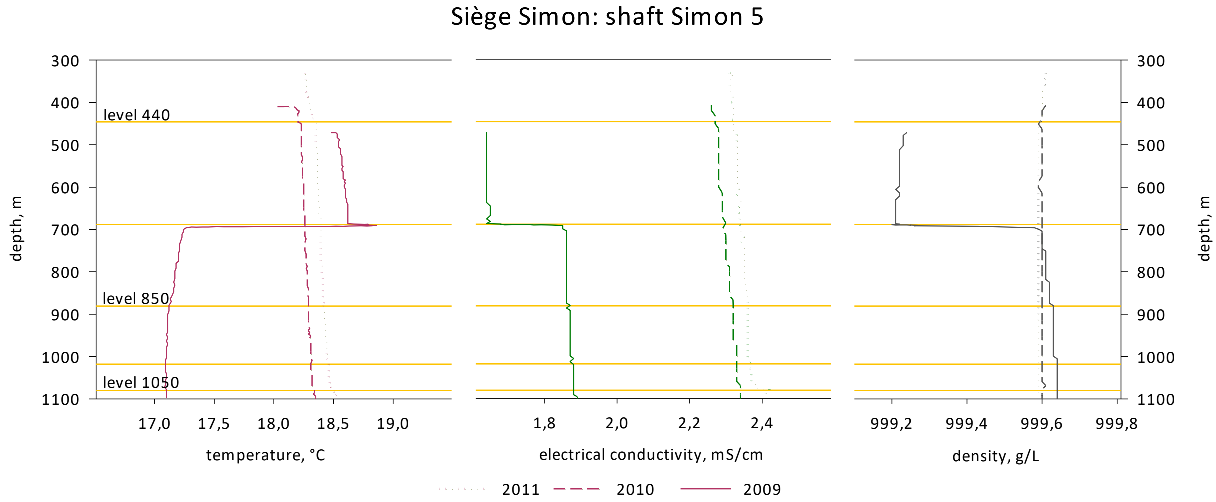

Figure S 4: Temperature profiles (measured), electrical conductivity profiles (measured) and density profiles (calculated with UNESCO equation) of the flooded Simon 5 shaft at the Siège Merlebach (Simon) colliery in France.

Kukla and Jindřich colliery

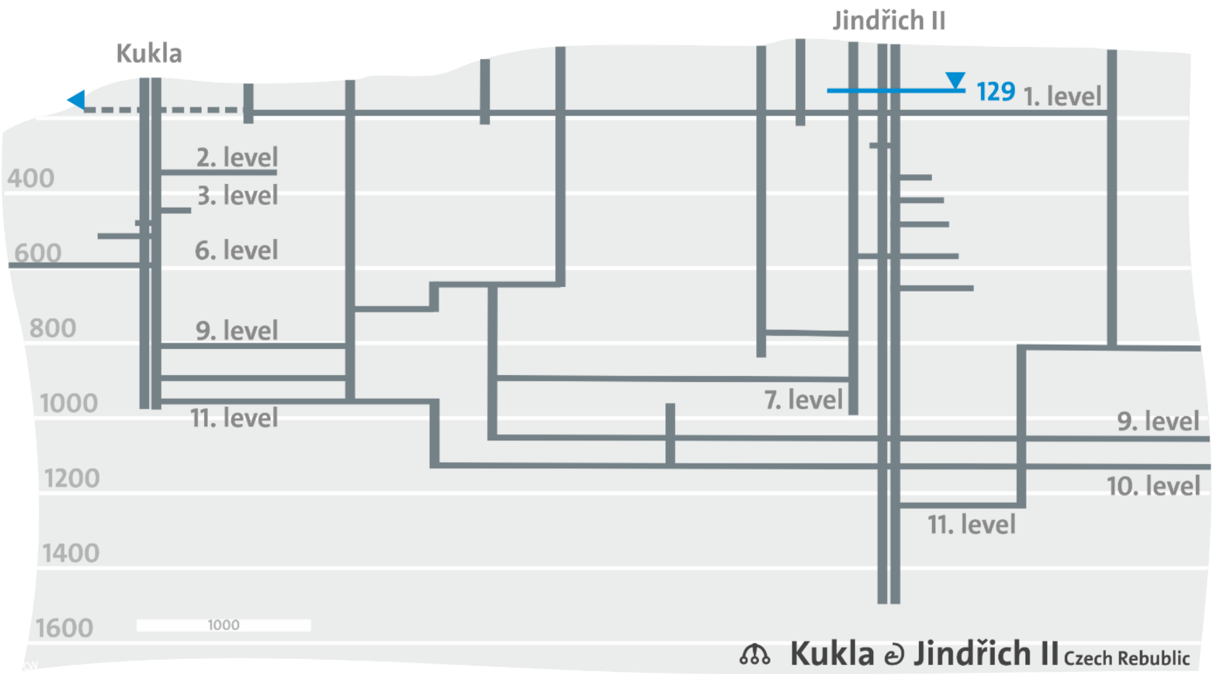

Figure S 5: Cross section of the Kukla and Jindřich colliery in Czech Republic.

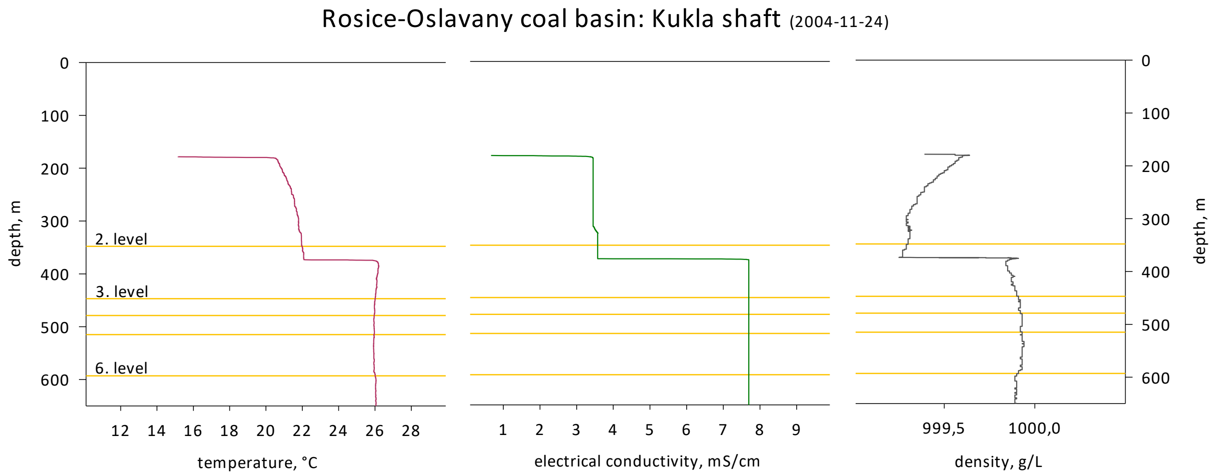

Figure S 6: Temperature profile (measured), electrical conductivity profile (measured) and density profile (calculated with UNESCO equation) of the flooded Kukla shaft at the Kukla colliery in Czech Republic. Levels accordingly to different available cross section.

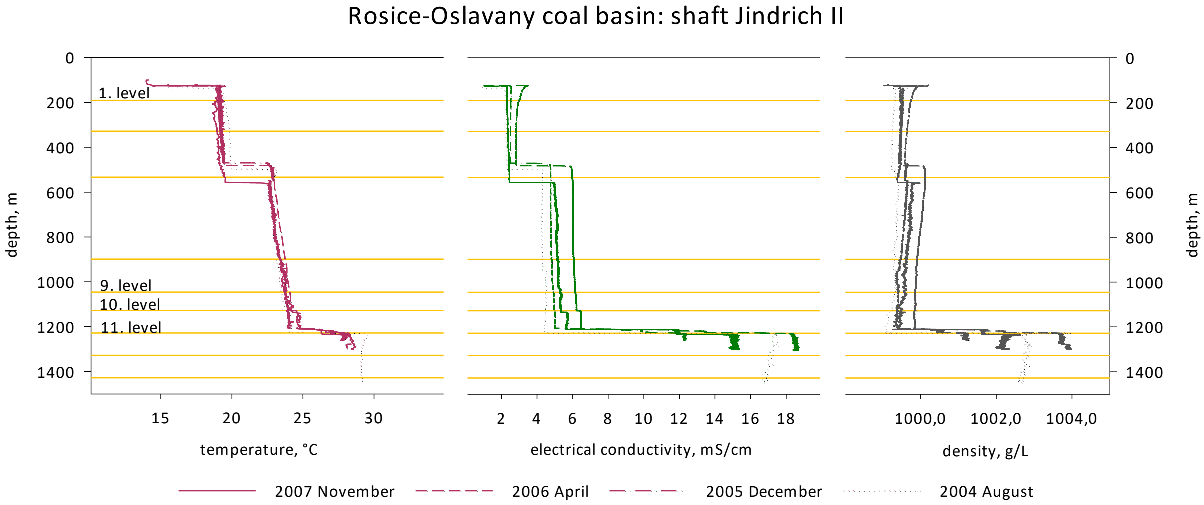

Figure S 7: Temperature profiles (measured), electrical conductivity profiles (measured) and density profiles (calculated with UNESCO equation) of the flooded Kukla shaft at the Jindřich II colliery in Czech Republic.

Hermann colliery

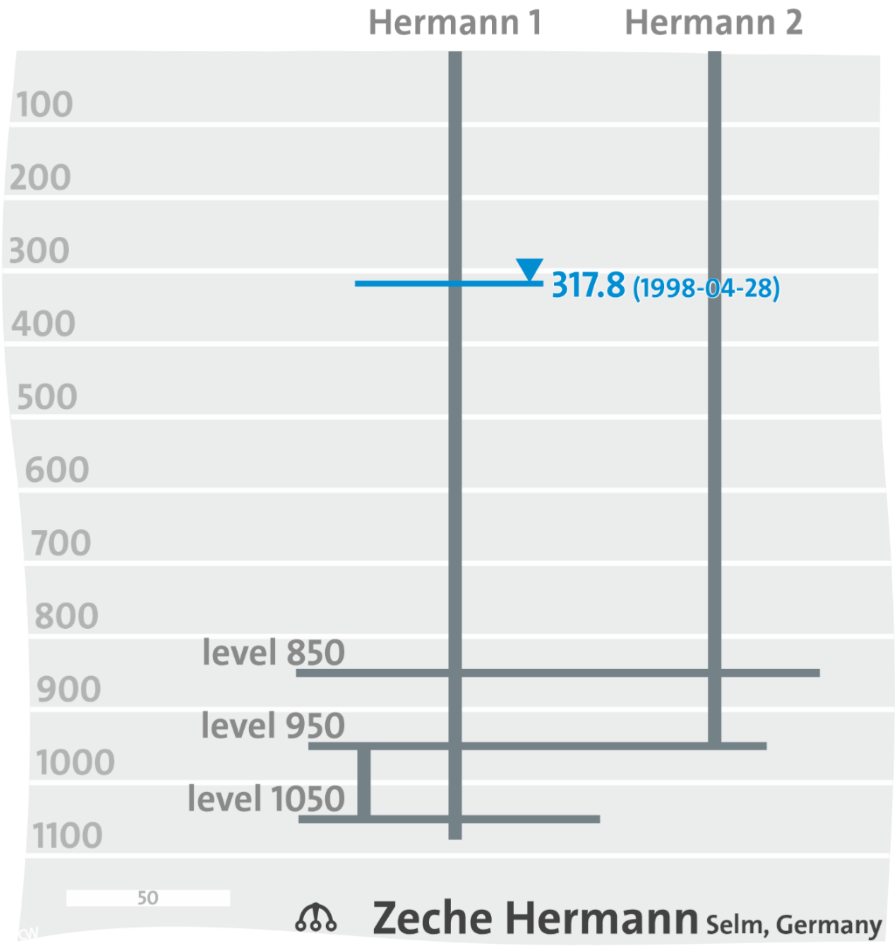

Figure S 8: Cross section of the Zeche Hermann colliery in Germany.

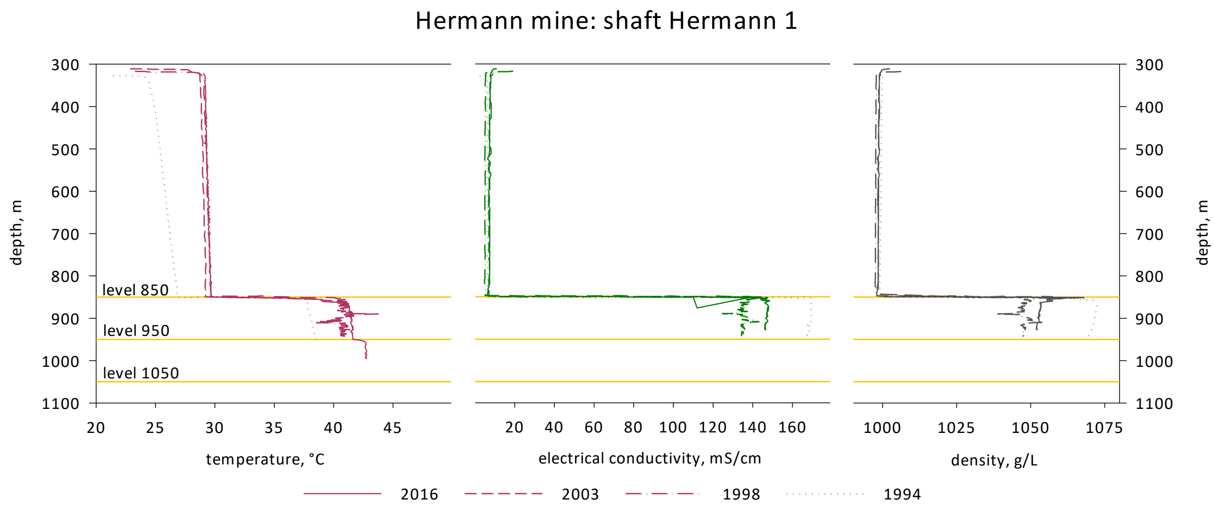

Figure S 9: Temperature profiles (measured), electrical conductivity profiles (measured) and density profiles (calculated with UNESCO equation) of the flooded Hermann 1 shaft at the Zeche Hermann colliery in Germany.

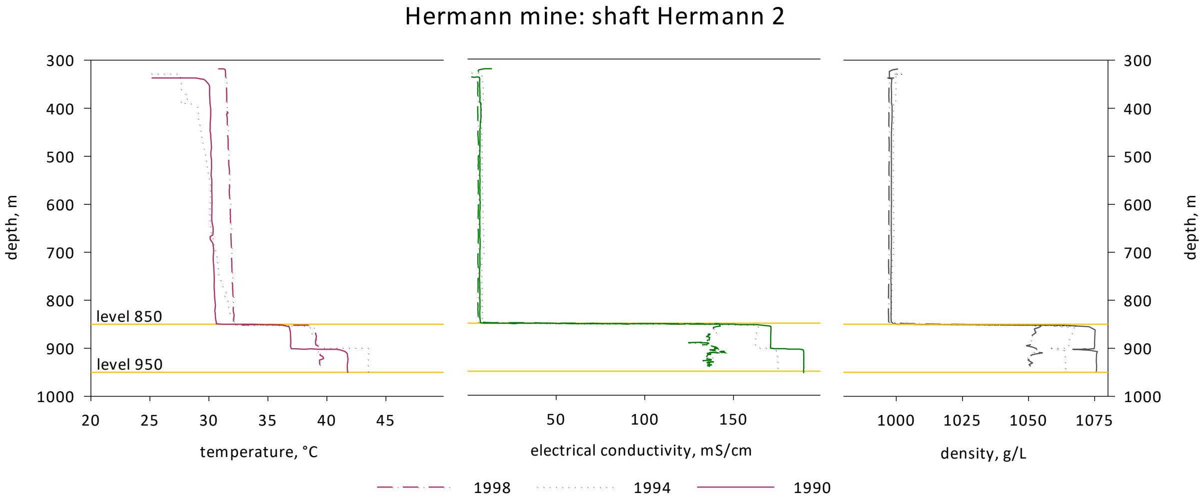

Figure S 10: Temperature profiles (measured), electrical conductivity profiles (measured) and density profiles (calculated with UNESCO equation) of the flooded Herman 2 shaft at the Zeche Hermann colliery in Germany.

Velsen colliery

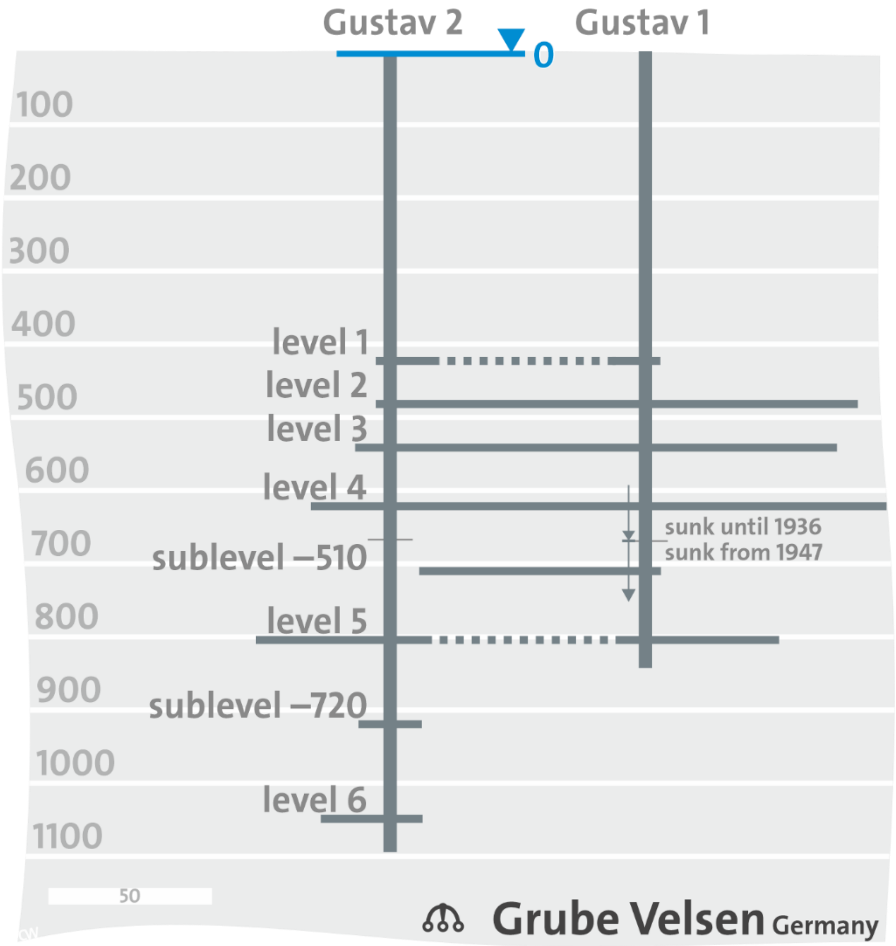

Figure S 11: Cross section of the Velsen colliery in Germany.

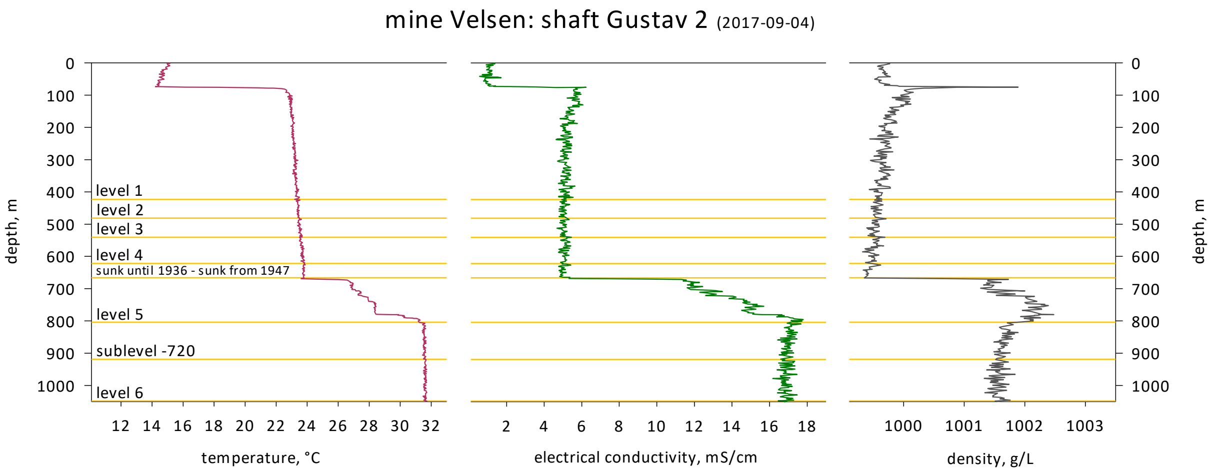

Figure S 12: Temperature profile (measured), electrical conductivity profile (measured) and density profile (calculated with UNESCO equation) of the flooded Gustav 2 shaft at the Velsen colliery in Germany.

Glückaufsegen colliery

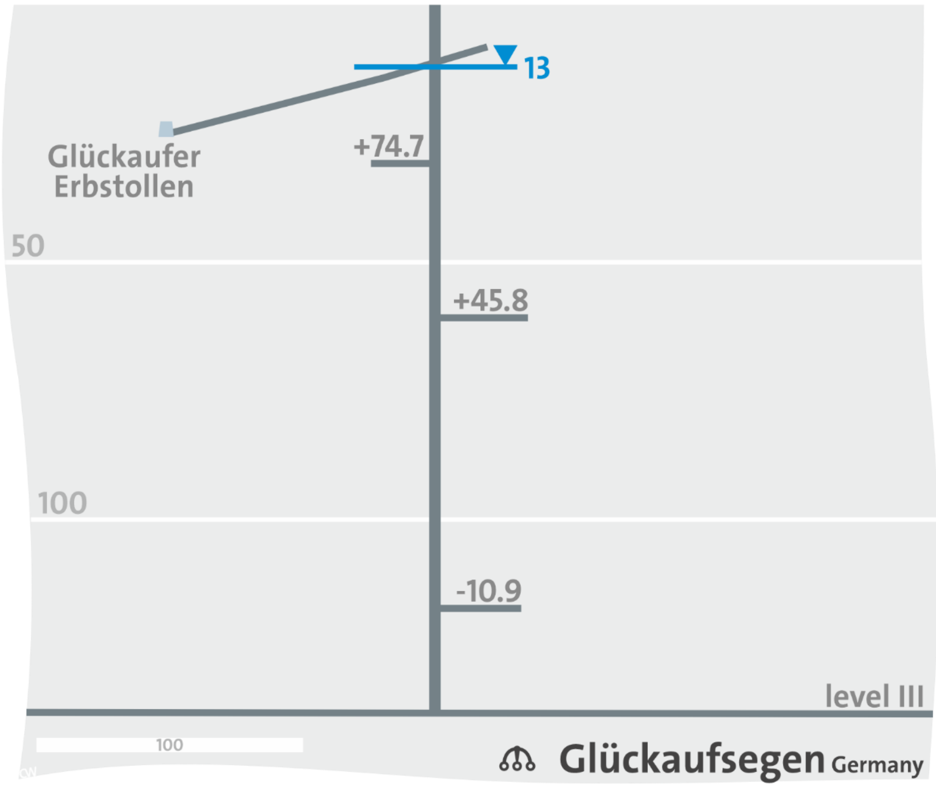

Figure S 13: Cross section of the Glückaufsegen colliery in Germany.

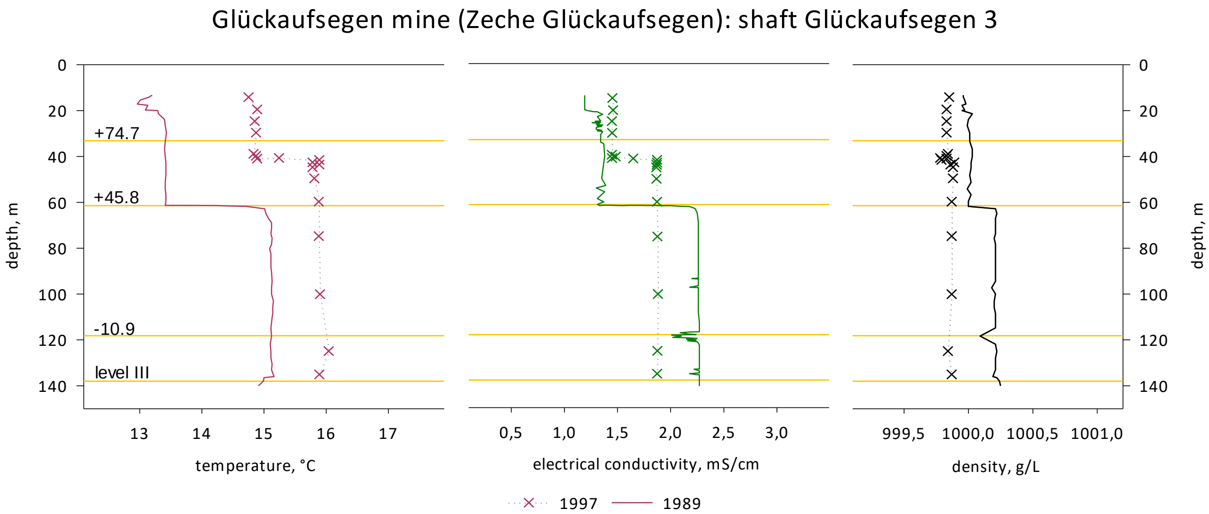

Figure S 14: Temperature profiles (measured), electrical conductivity profiles (measured) and density profiles (calculated with UNESCO equation) of the flooded Glückaufsegen 3 shaft at the Glückaufsegen colliery in Germany.

Friedlicher Nachbar colliery

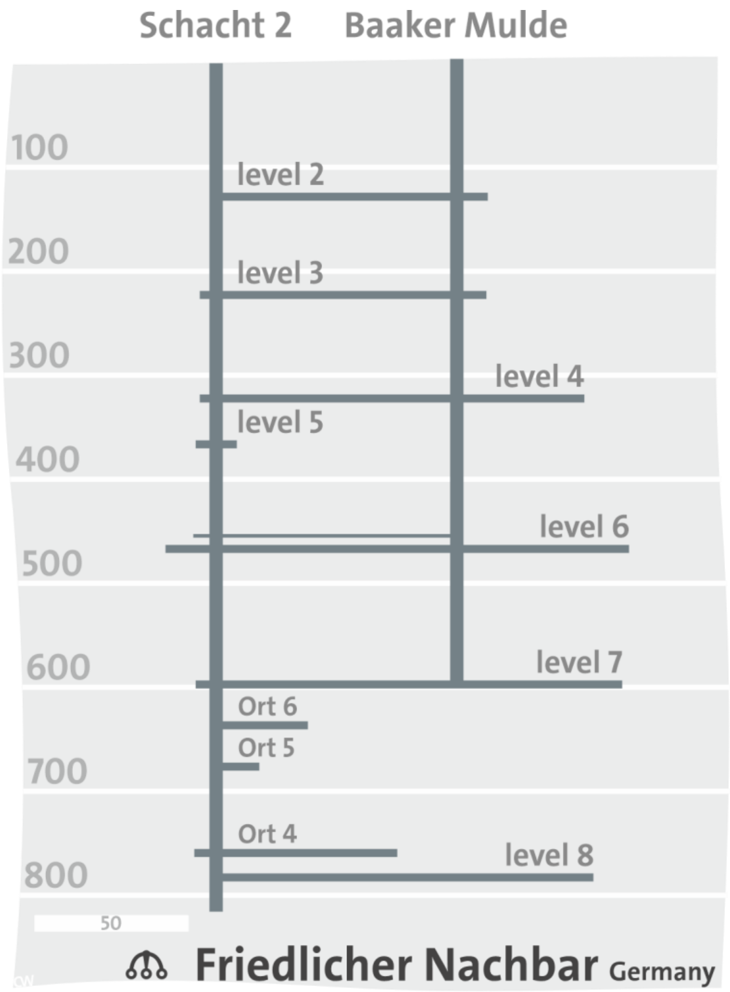

Figure S 15: Cross section of the Friedlicher Nachbar colliery in Germany.

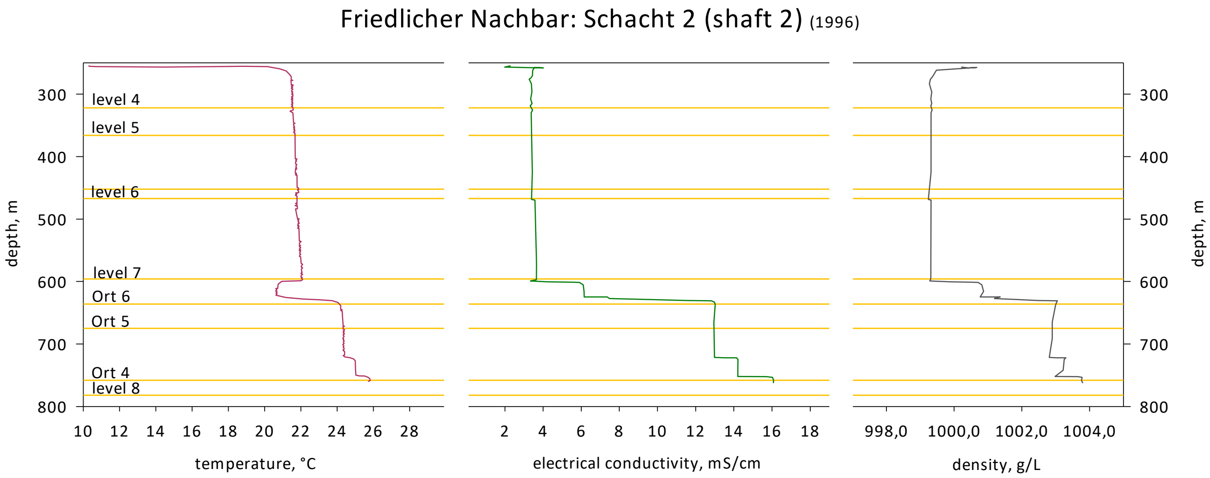

Figure S 16: Temperature profile (measured), electrical conductivity profile (measured) and density profile (calculated with UNESCO equation) of the flooded shaft 2 at the Friedlicher Nachbar colliery in Germany.

San Vincente colliery

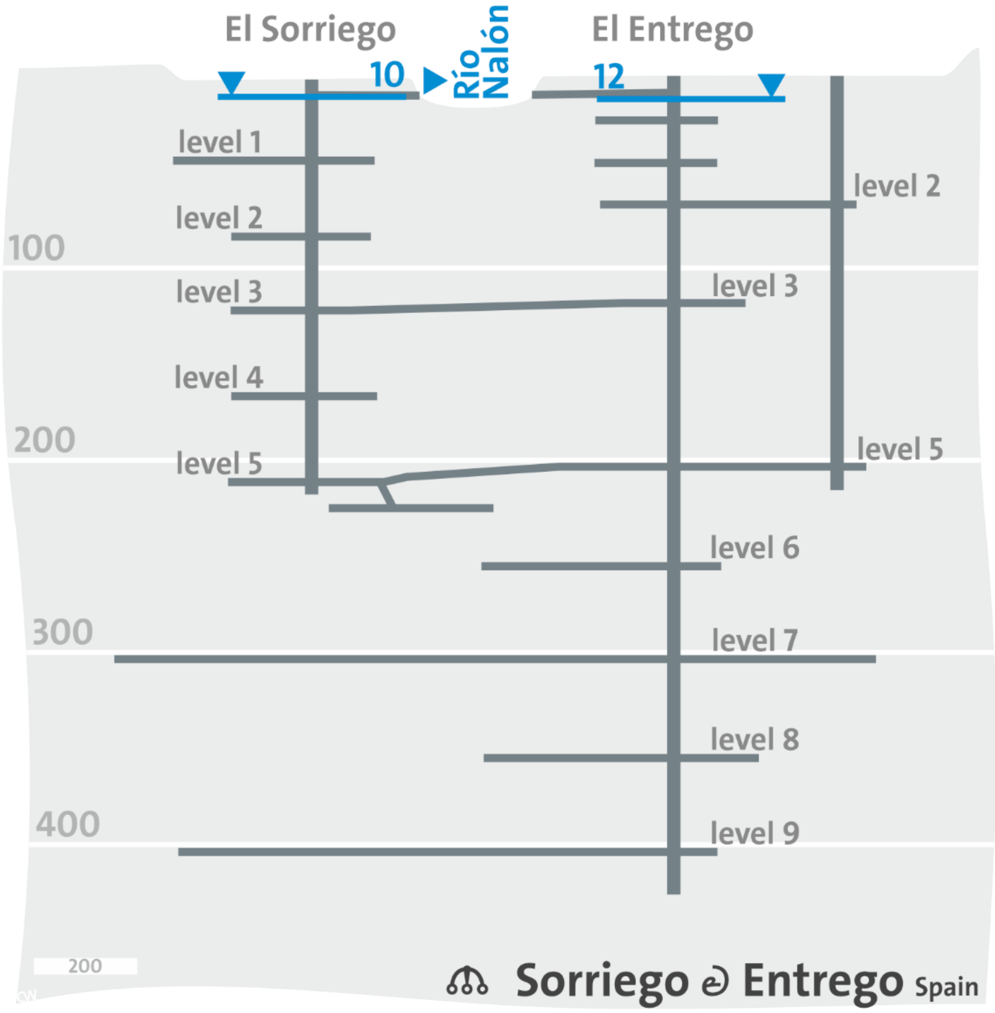

Figure S 17: Cross section of the San Vincente colliery in Spain.

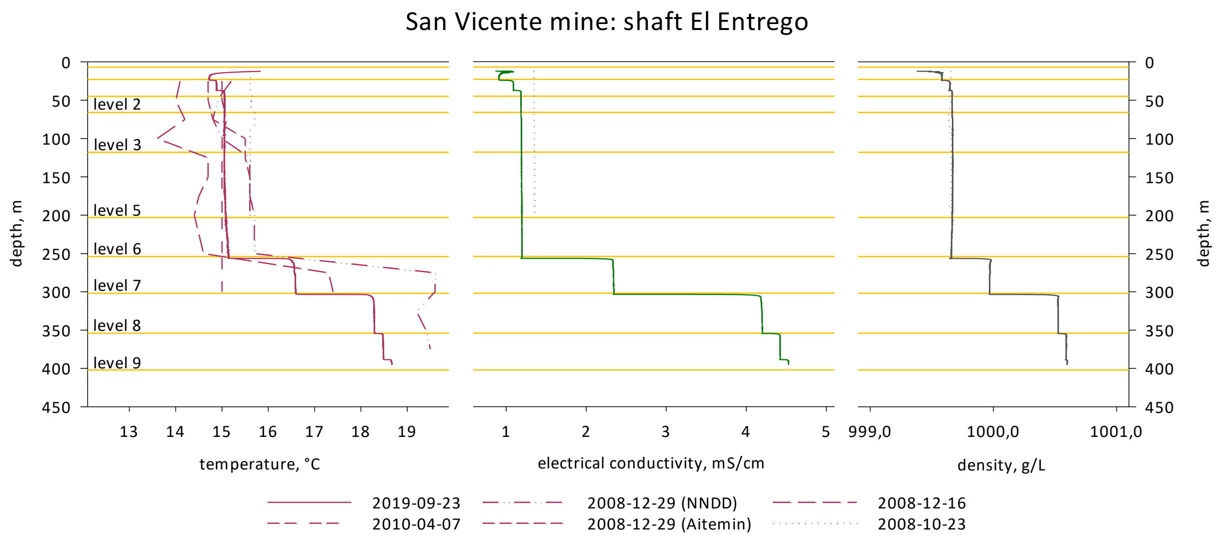

Figure S 18: Temperature profiles (measured), electrical conductivity profiles (measured) and density profiles (calculated with UNESCO equation) of the flooded El Entrego shaft at the San Vincente colliery in Spain.

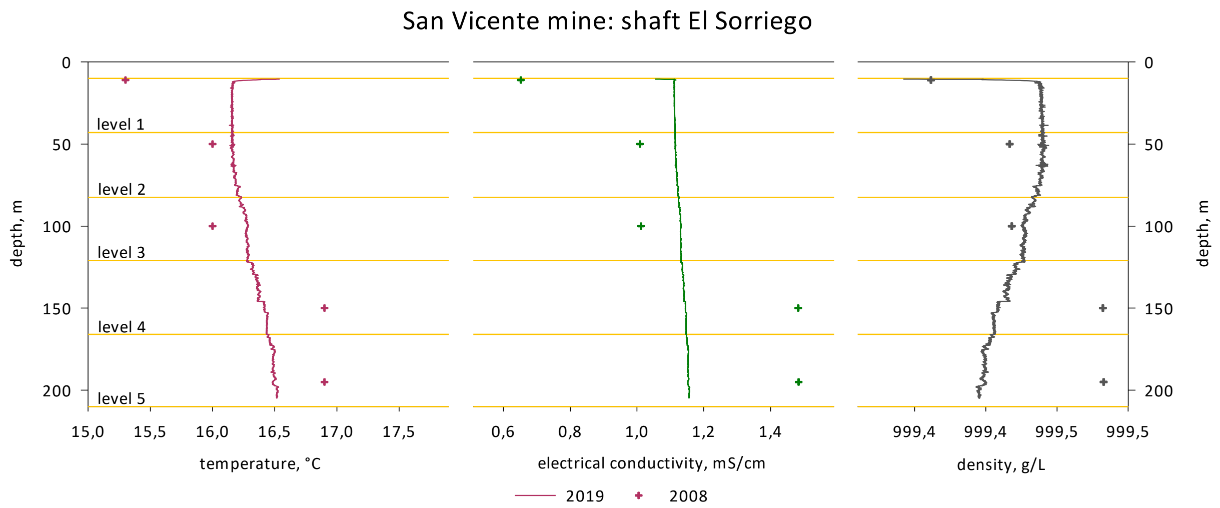

Figure S 19: Temperature profiles (measured), electrical conductivity profiles (measured) and density profiles (calculated with UNESCO equation) of the flooded El Sorriego shaft at the San Vincente colliery in Spain.

Horden colliery

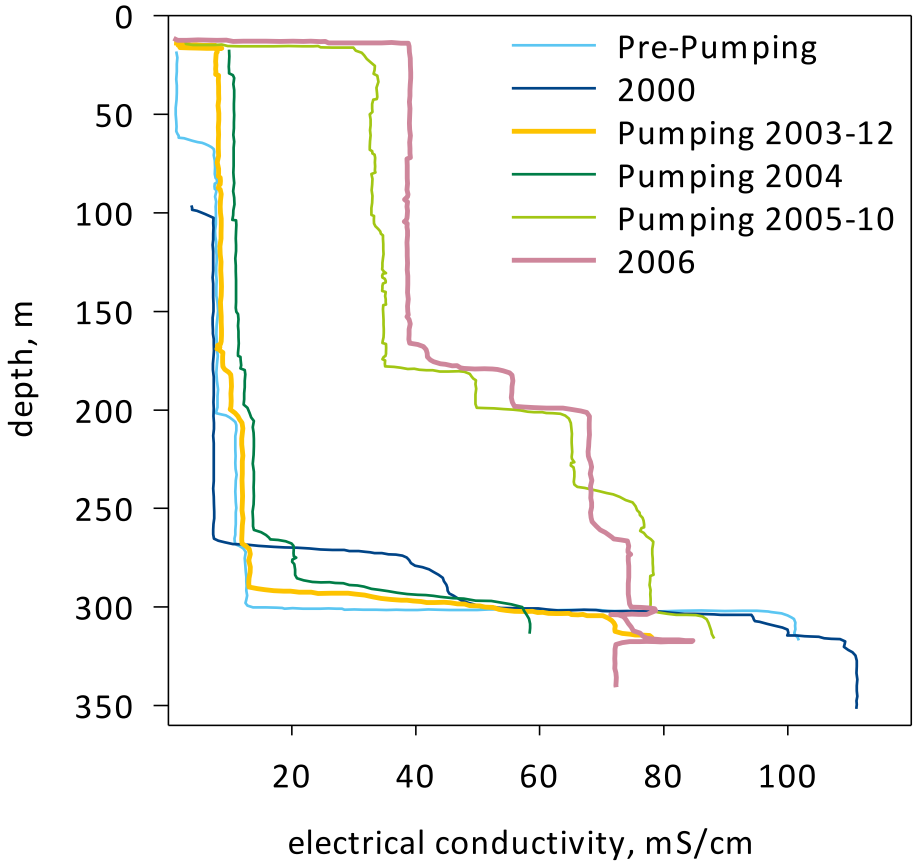

Figure S 20: Electrical conductivity profile (measured) of the flooded S40 Horden South Shaft at the Horden colliery in Great Britain. Reproduced with the permission of © The Coal Authority 2024. All rights reserved.

Merkur lead mine

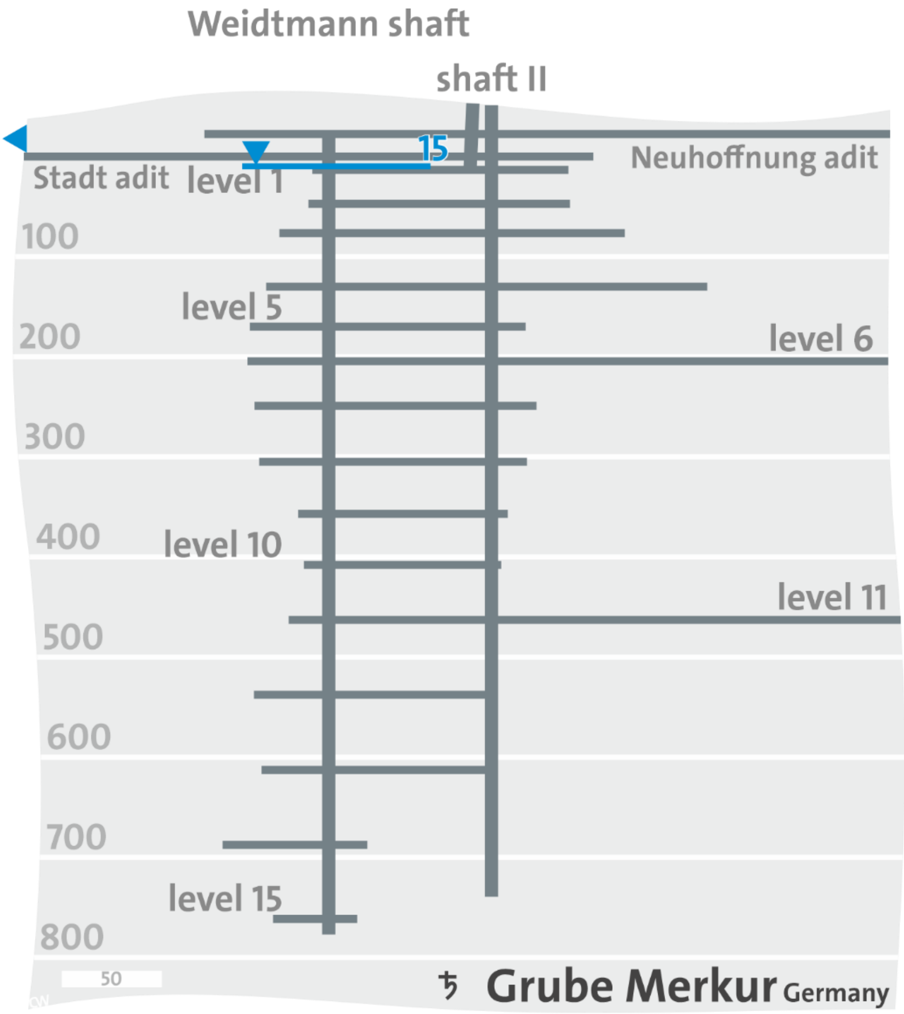

Figure S 21: Cross section of the Merkur lead mine in Germany.

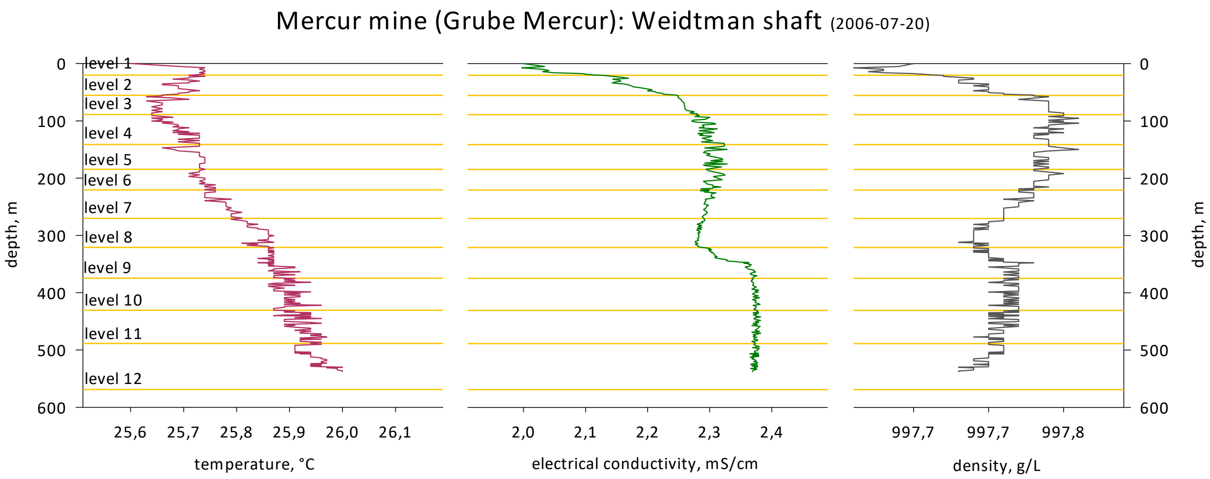

Figure S 22: Temperature profile (measured), electrical conductivity profile (measured) and density profile (calculated with UNESCO equation) of the flooded Weidtman shaft at the Merkur lead mine in Germany.

Straßberg fluorspar mine

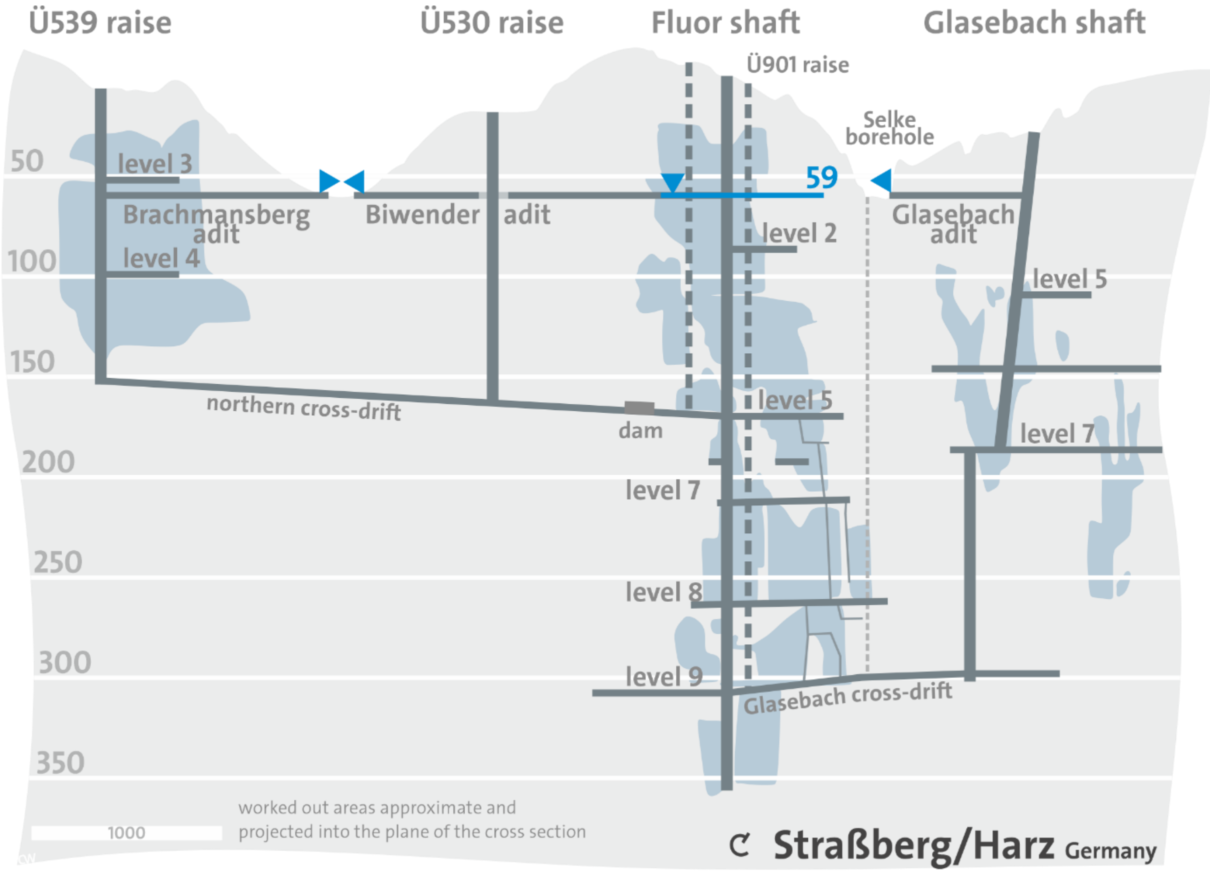

Figure S 23: Cross section of the Straßberg fluorspar mine in Germany.

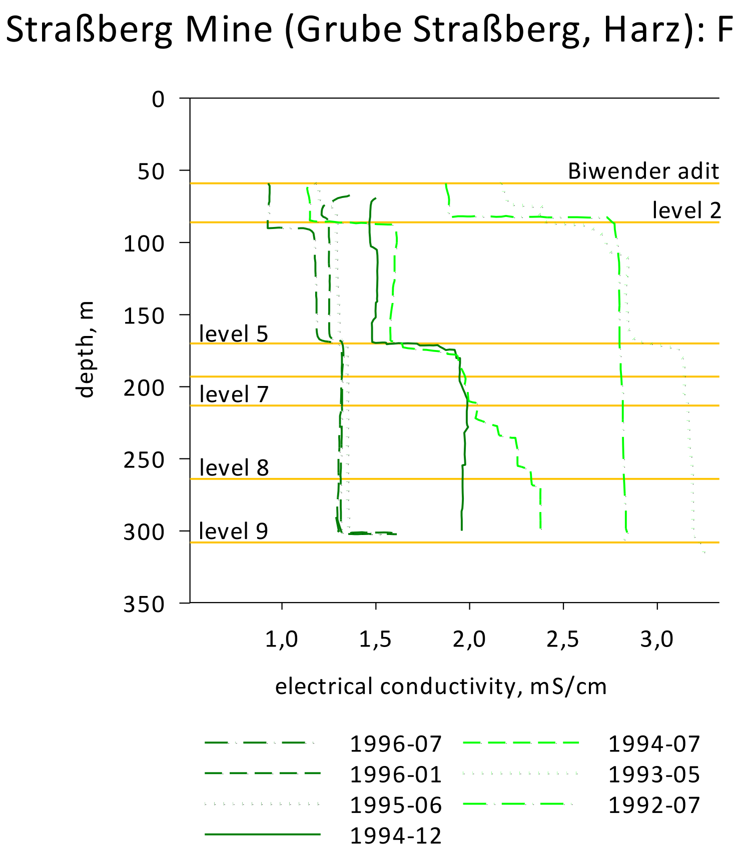

Figure S 24: Electrical conductivity profiles (measured) of the flooded Flour shaft at the Straßberg fluorspar mine in Germany.

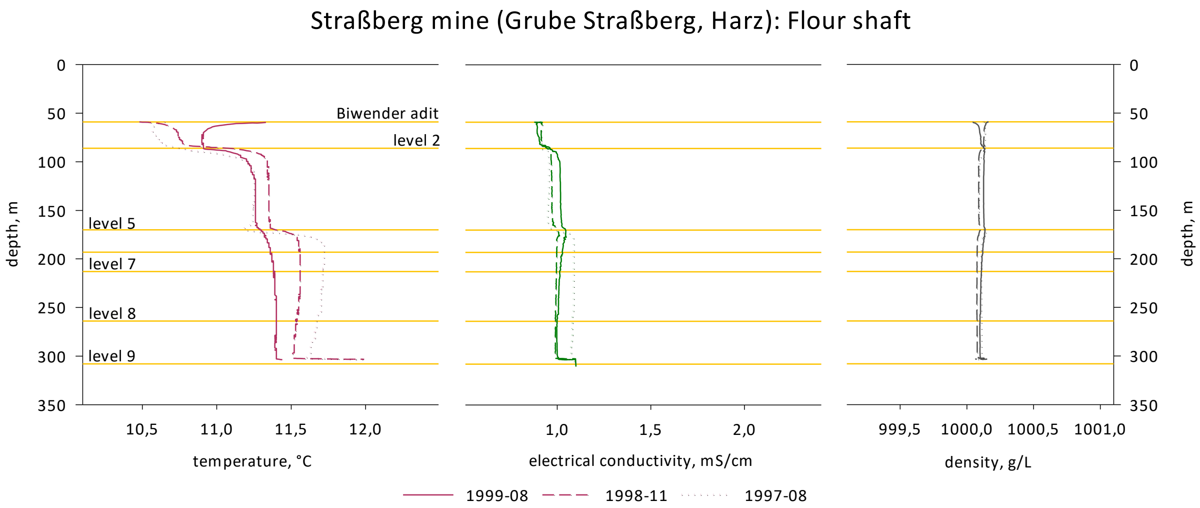

Figure S 25: Temperature profiles (measured), electrical conductivity profiles (measured) and density profiles (calculated with UNESCO equation) from 1997, 1998 and 1999 of the flooded Flour shaft at the Straßberg fluorspar mine in Germany.

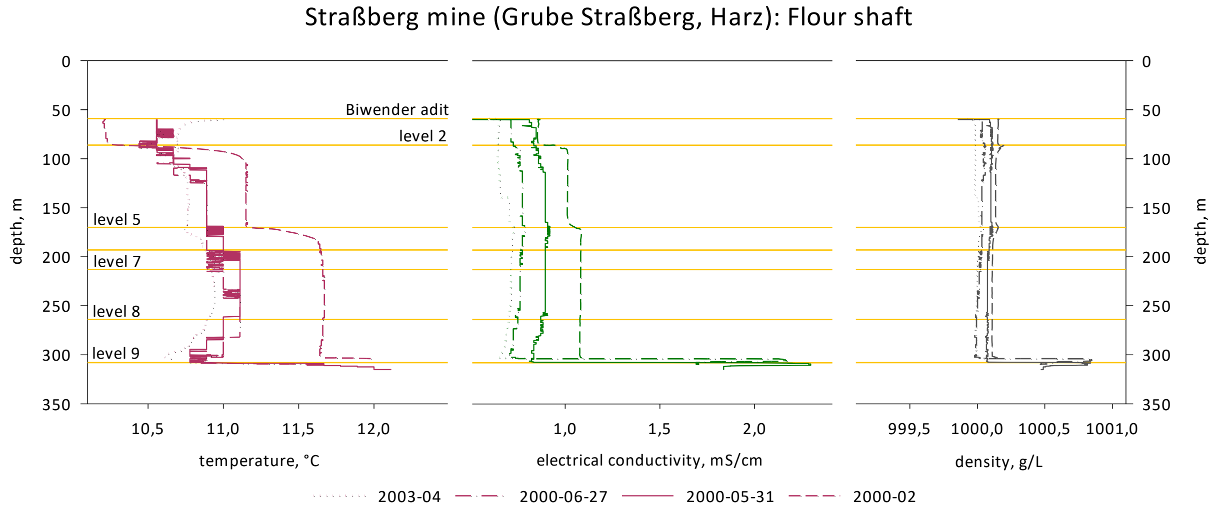

Figure S 26: Temperature profiles (measured), electrical conductivity profiles (measured) and density profiles (calculated with UNESCO equation) from 2000 and 2003 of the flooded Flour shaft at the Straßberg fluorspar mine in Germany.

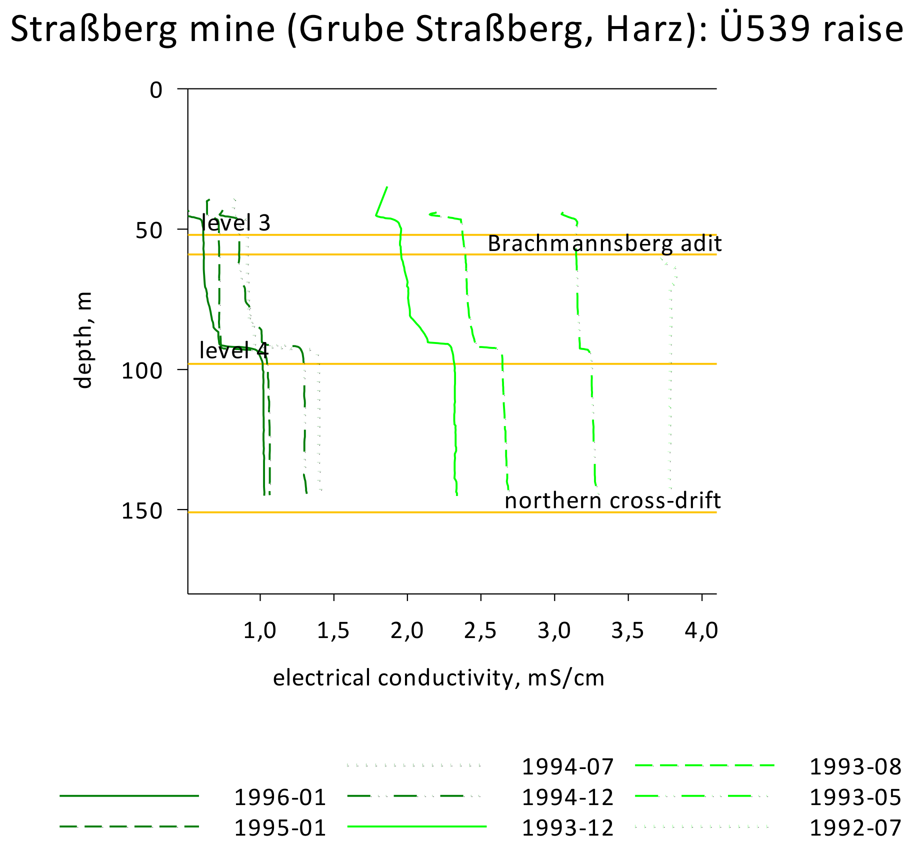

Figure S 27: Electrical conductivity profiles (measured) of the flooded Ü539 raise at the Straßberg fluorspar mine in Germany.

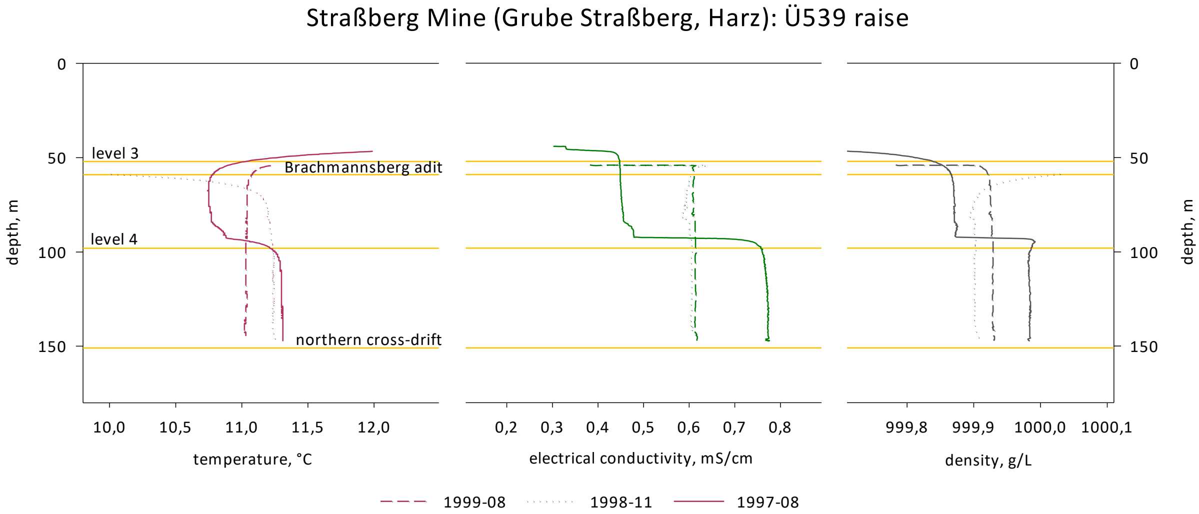

Figure S 28: Temperature profiles (measured), electrical conductivity profiles (measured) and density profiles (calculated with UNESCO equation) from 1997, 1998 and 1999 of the flooded Ü539 raise at the Straßberg fluorspar mine in Germany.

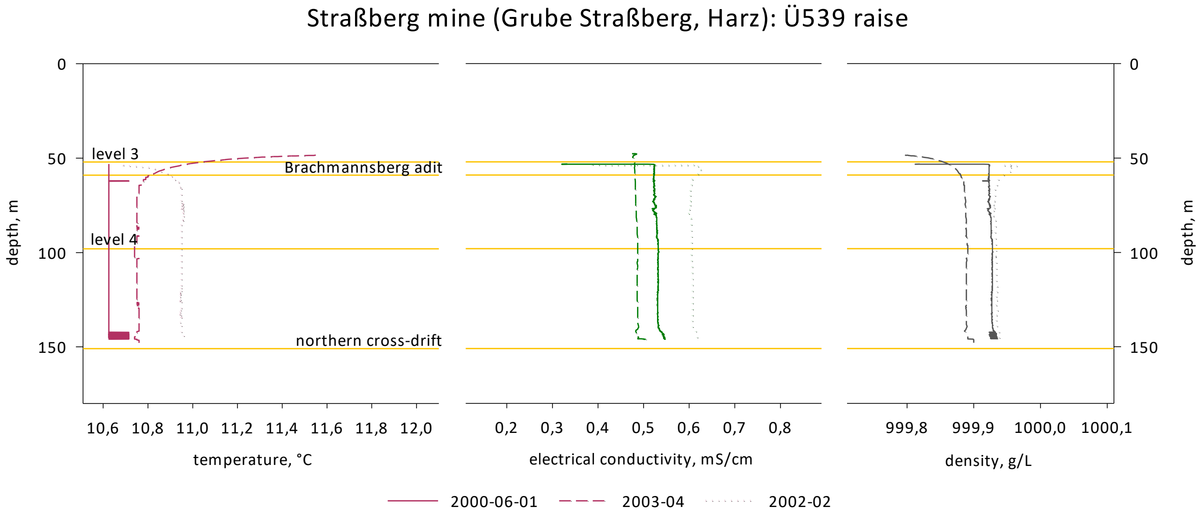

Figure S 29: Temperature profiles (measured), electrical conductivity profiles (measured) and density profiles (calculated with UNESCO equation) from 2000, 2002 and 2003 of the flooded Ü539 raise at the Straßberg fluorspar mine in Germany.

Meggen mine

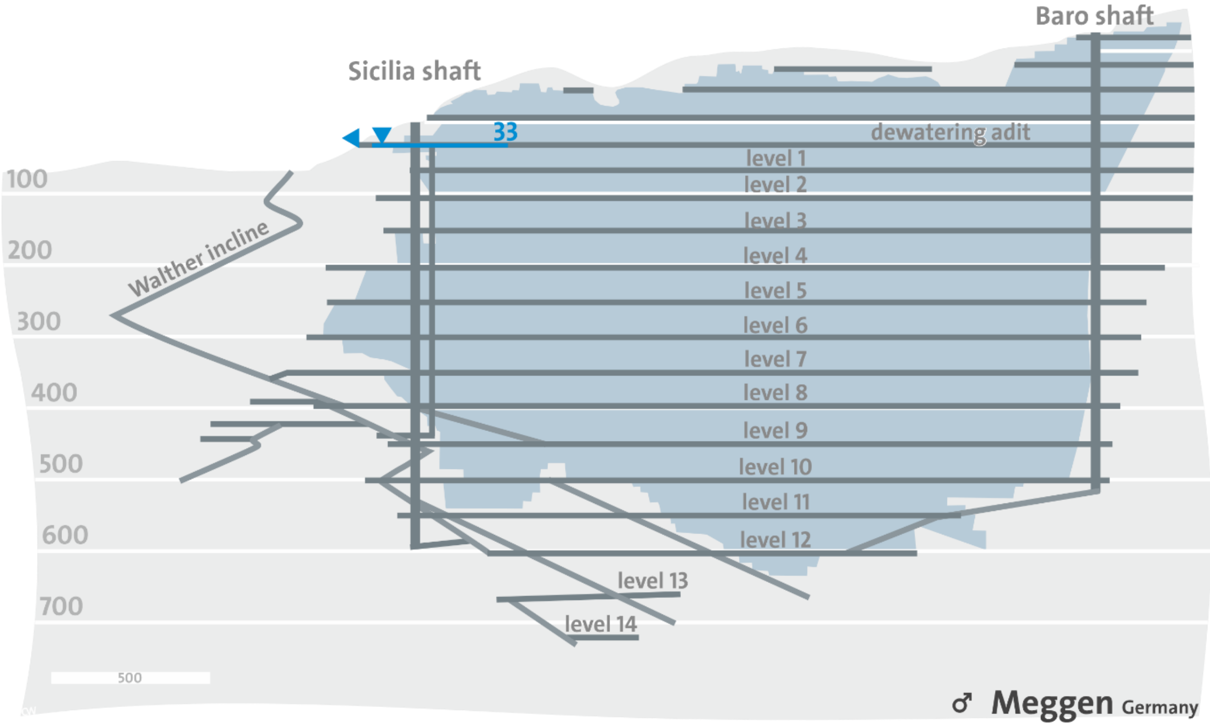

Figure S 30: Cross section of the polymetallic Meggen mine in Germany.

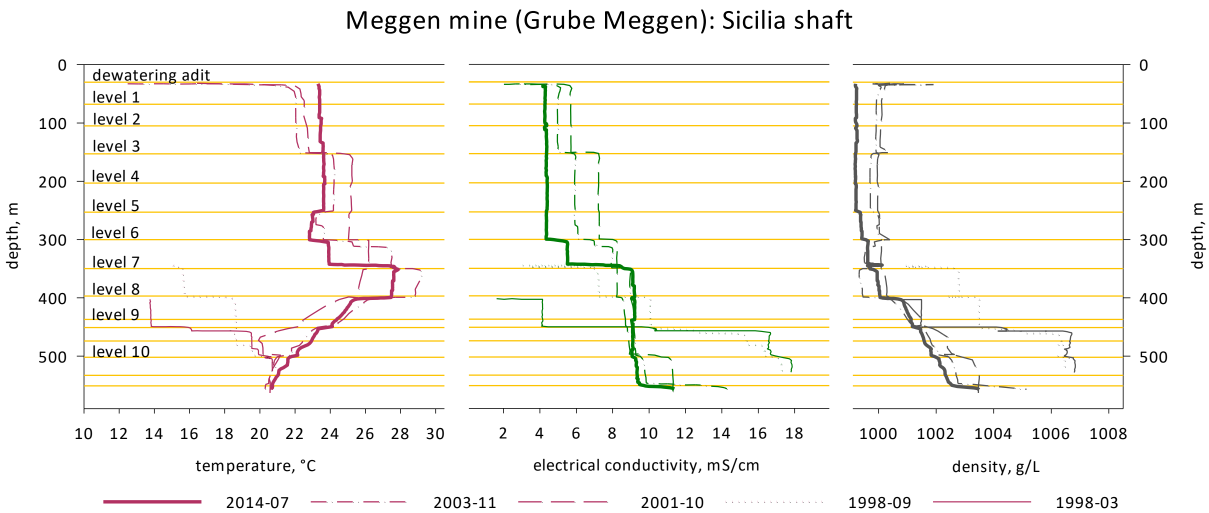

Figure S 31: Temperature profiles (measured), electrical conductivity profiles (measured) and density profiles (calculated with UNESCO equation) of the flooded Sicilia shaft at the polymetallic Meggen mine in Germany.

West Rand gold mine #8 Shaft

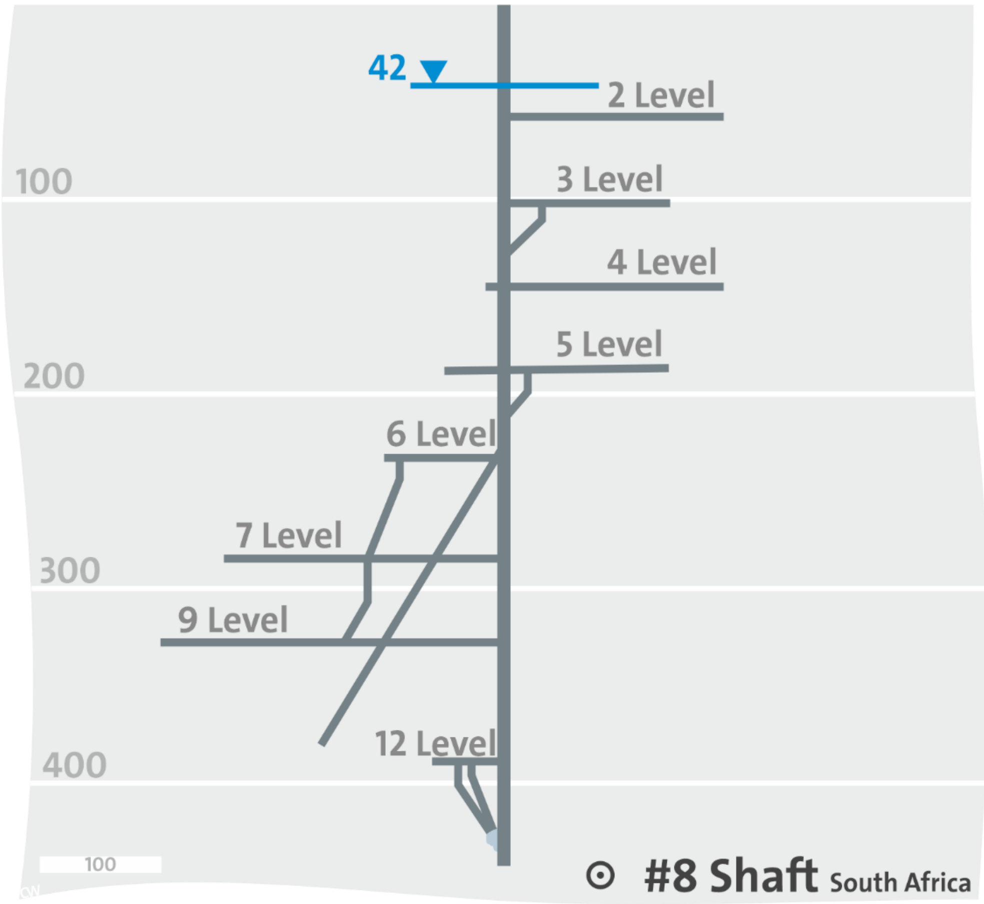

Figure S 32: Cross section of the West Rand gold mine #8 Shaft in South Africa.

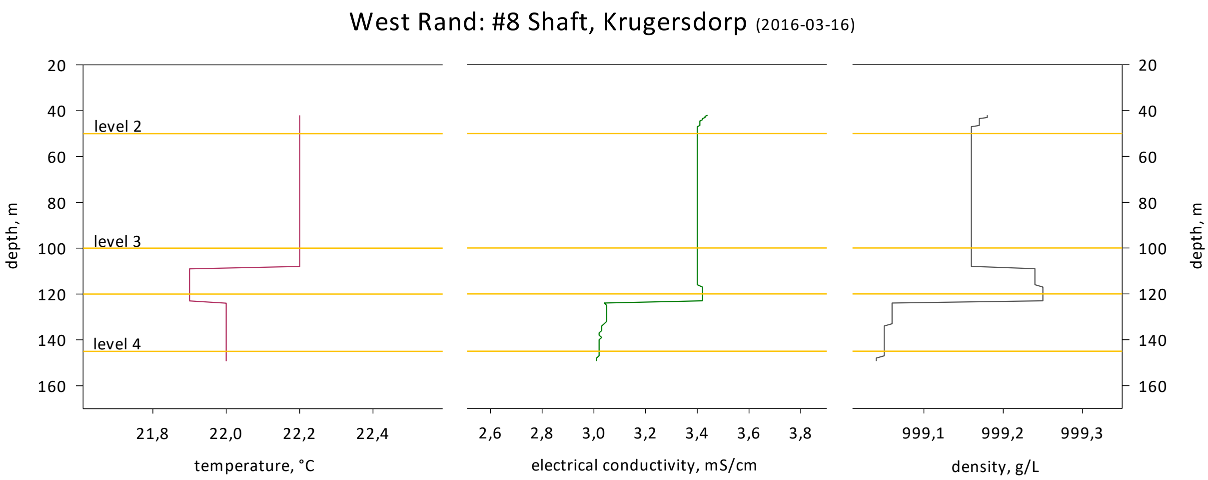

Figure S 33: Temperature profile (measured), electrical conductivity profile (measured) and density profile (calculated with UNESCO equation) of the flooded #8 Shaft at the West Rand gold mine #8 Shaft in South Africa.

Leopold-Louise iron ore mine

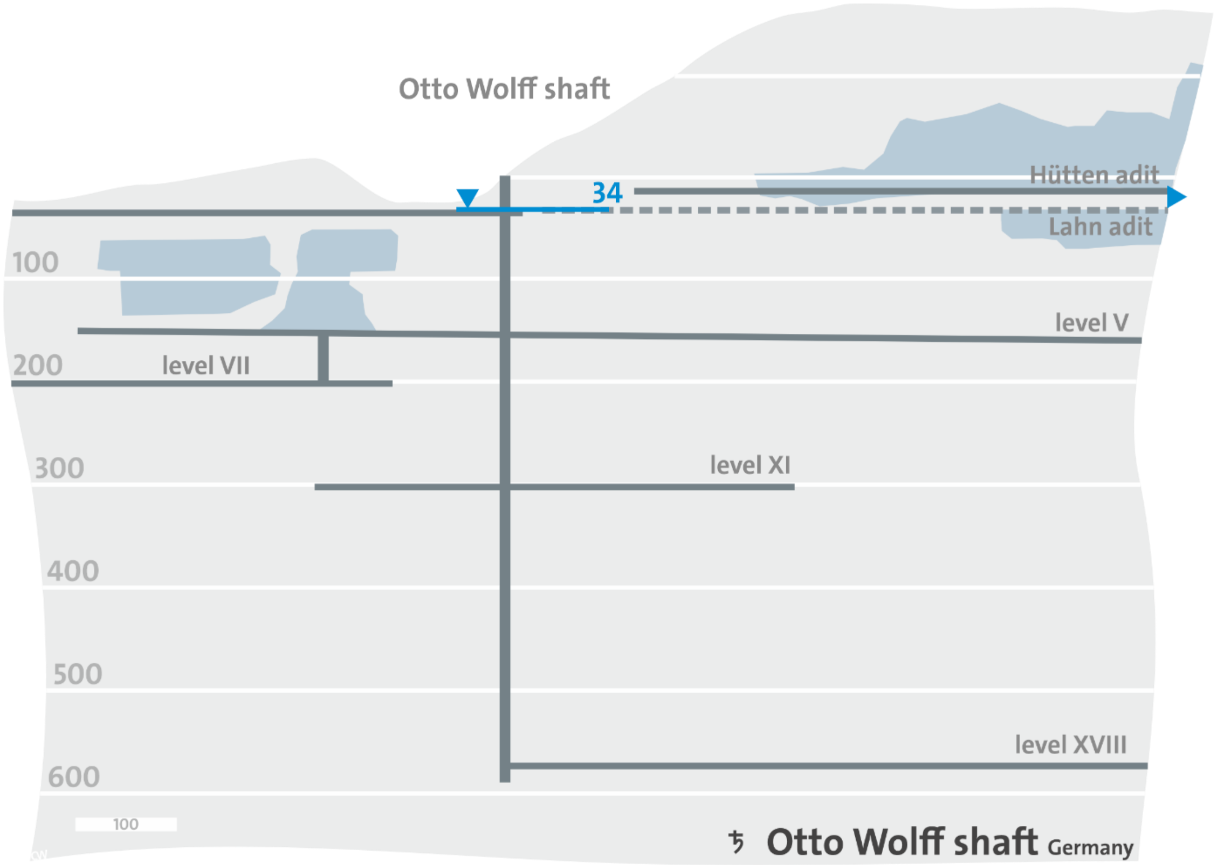

Figure S 34: Cross section of the Leopold-Louise iron ore mine in Germany.

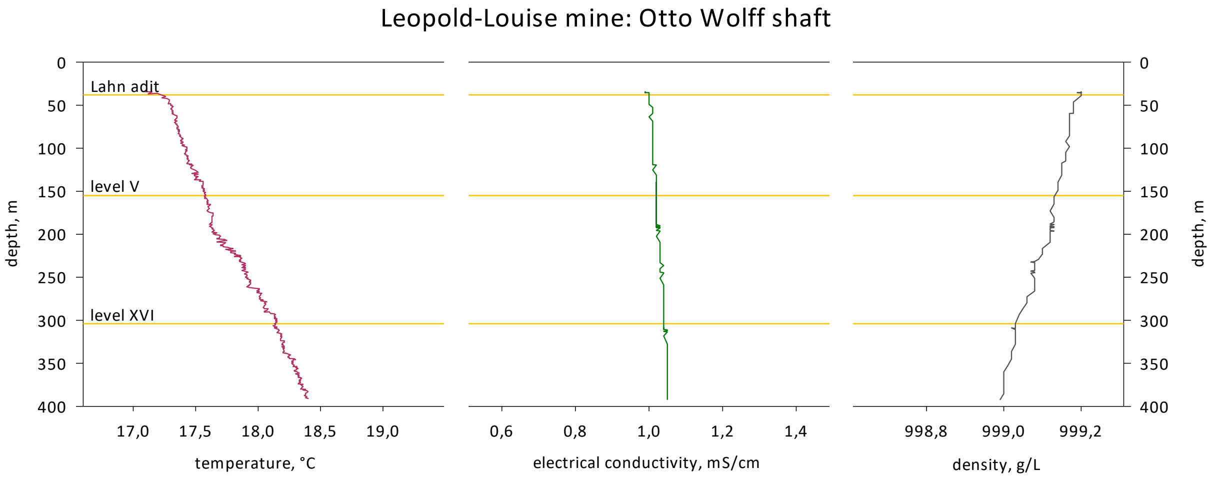

Figure S 35: Temperature profile (measured), electrical conductivity profile (measured) and density profile (calculated with UNESCO equation) of the flooded Otto Wolff shaft at the Leopold-Louise iron ore mine in Germany.

Hancock copper mine

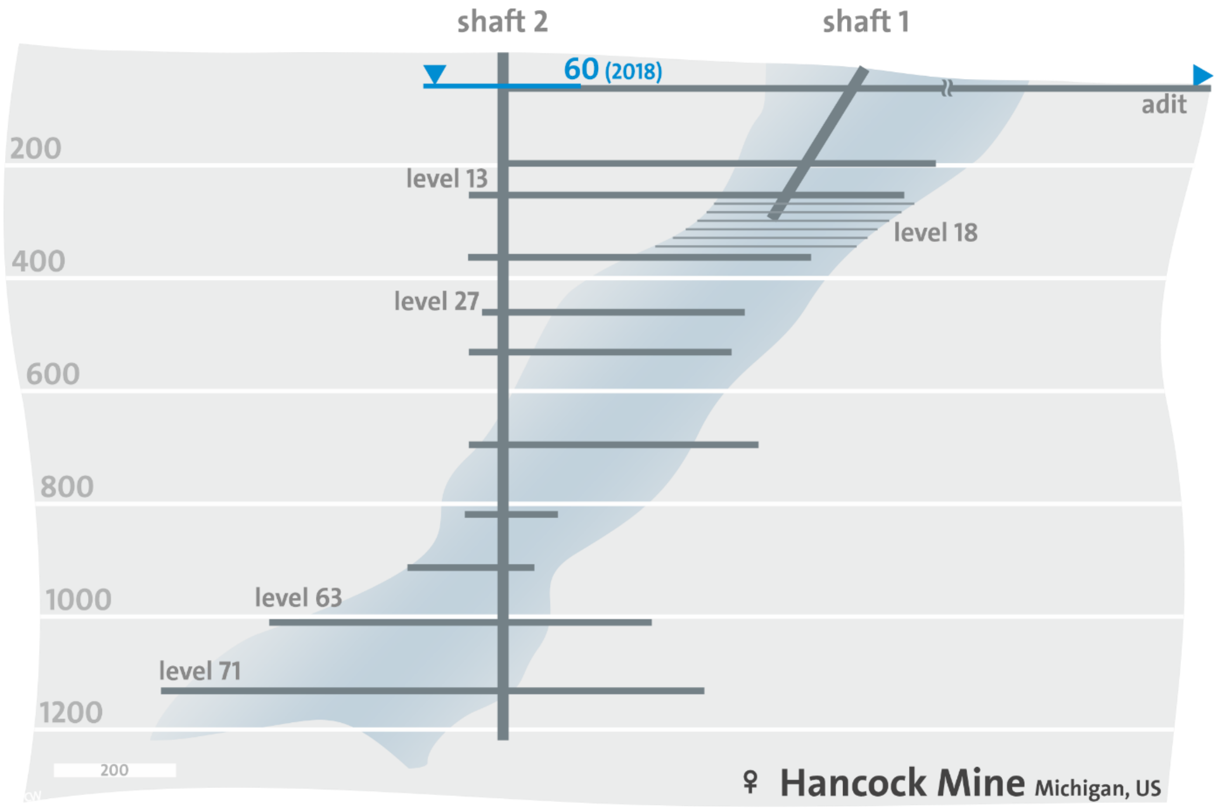

Figure S 36: Cross section of the Hancock copper mine in the United States of America.

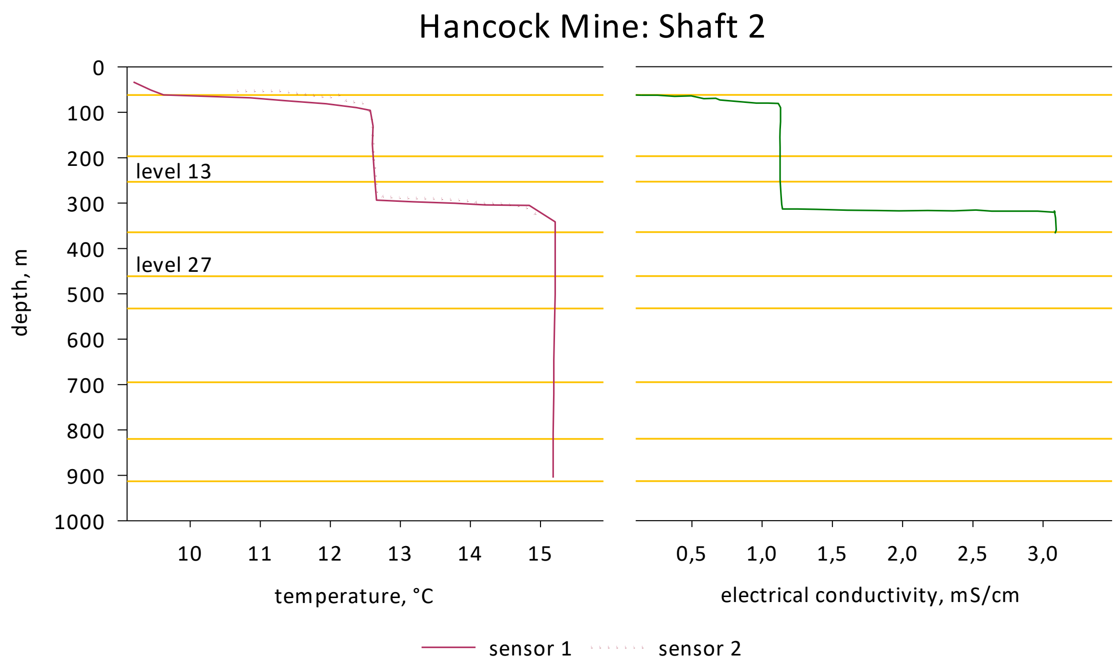

Figure S 37: Temperature profiles (measured) and electrical conductivity profile (measured) of flooded shaft 2 at the Hancock copper mine in the United States of America.

Georg iron ore mine

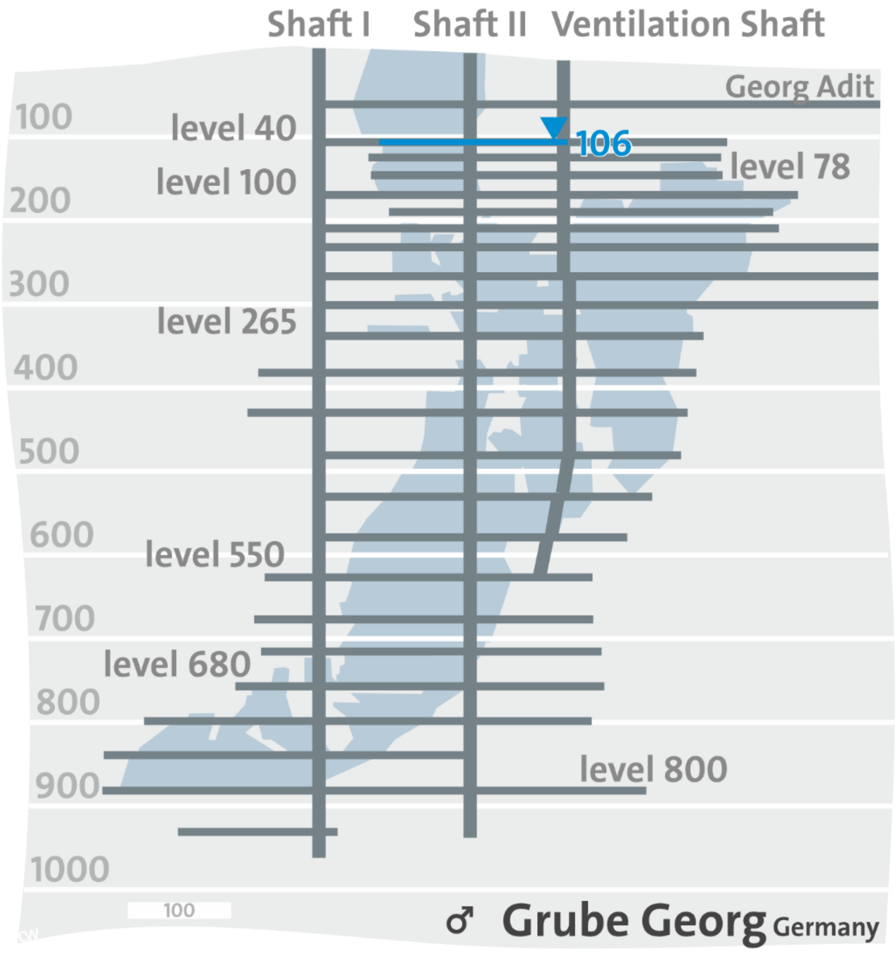

Figure S 38: Cross section of the Georg iron ore mine in Germany.

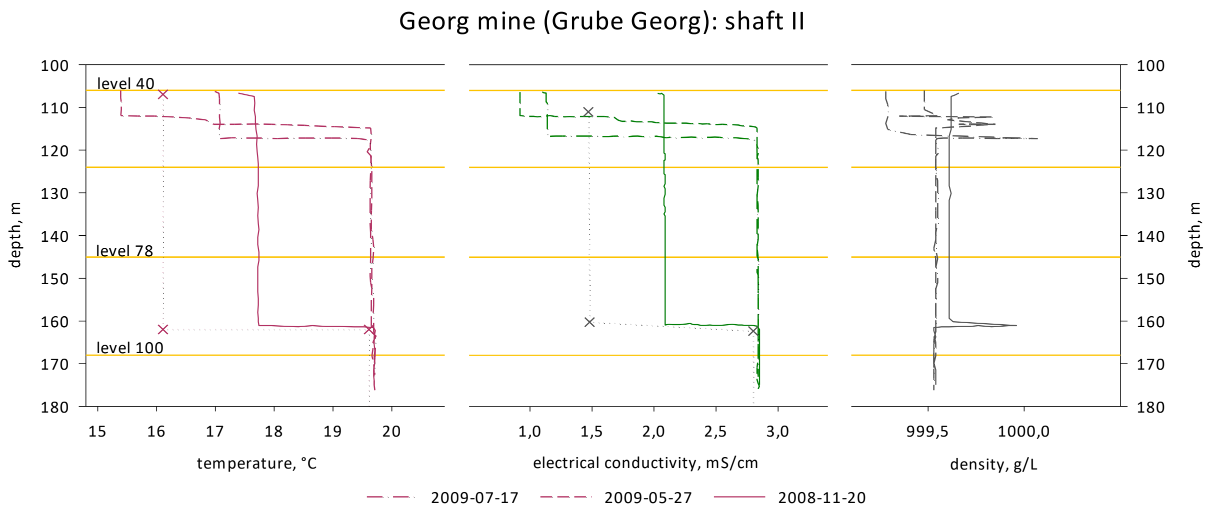

Figure S 39: Temperature profiles (measured), electrical conductivity profiles (measured) and density profiles (calculated with UNESCO equation) of the flooded shaft II at the Georg iron ore mine in Germany.

Stahlberg iron ore

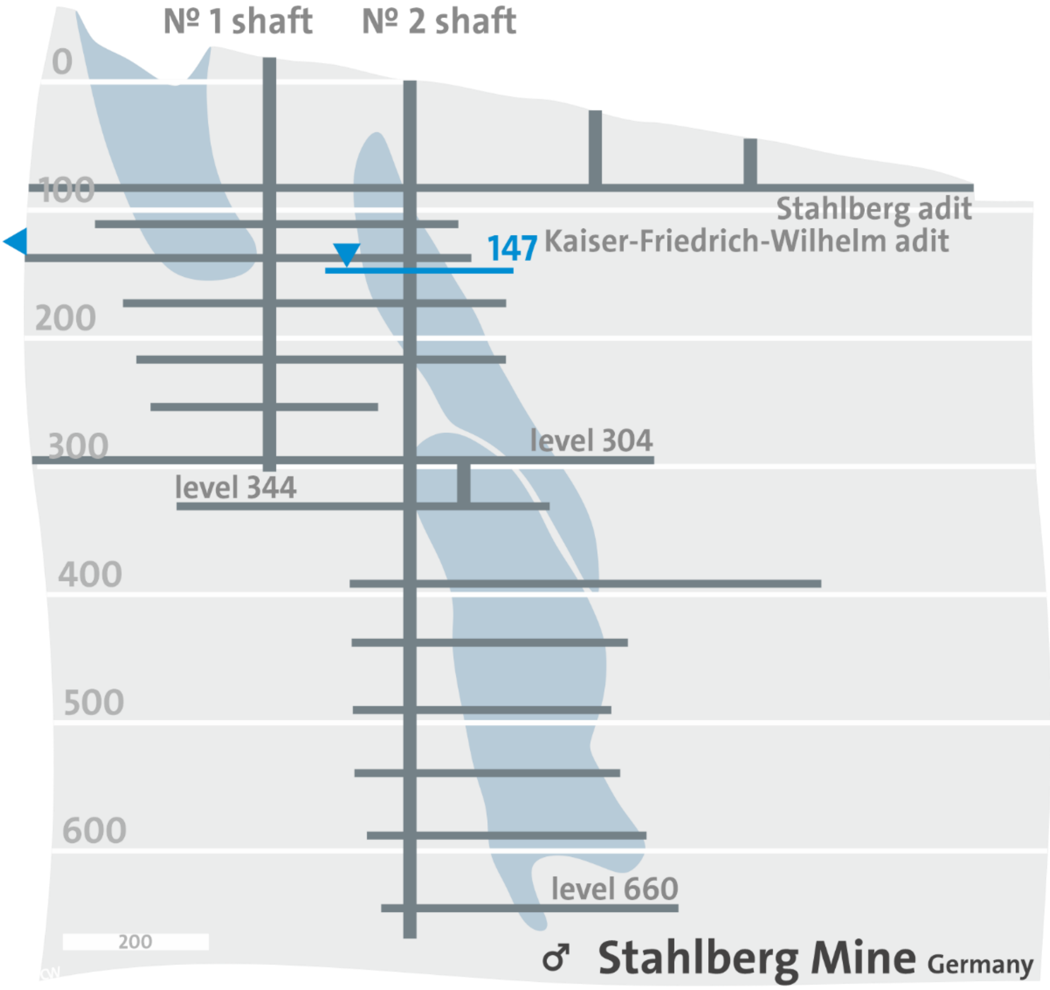

Figure S 40: Cross section of the Stahlberg iron ore mine in Germany.

Stahlberg mine (Grube Stahlberg): No 2 shaft (2000)

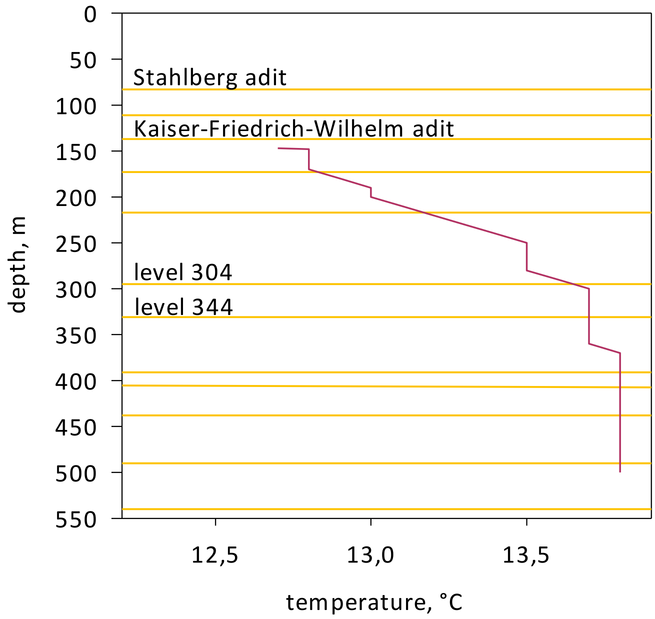

Figure S 41: Temperature profile (measured) of flooded shaft 2 at the Stahlberg iron ore mine in Germany.

Urgeiriça uranium mine

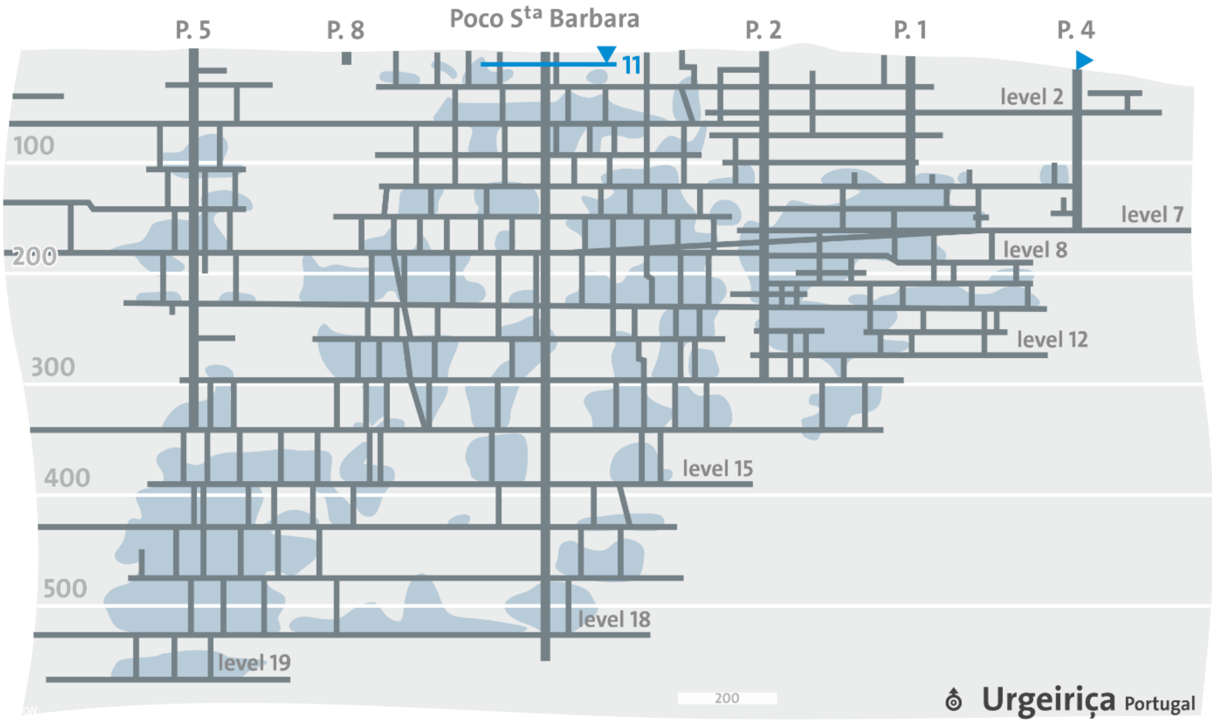

Figure S 42: Cross section of the Urgeiriça uranium mine in Portugal.

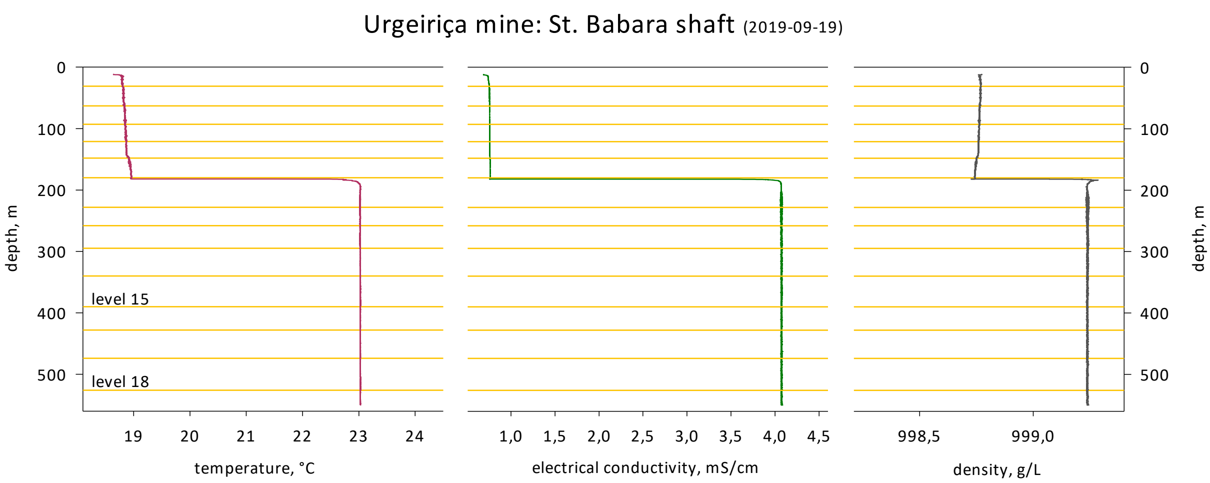

Figure S 43: Temperature profile (measured), electrical conductivity profile (measured) and density profile (calculated with UNESCO equation) of the flooded St Barbara shaft at the Urgeiriça uranium mine in Portugal.

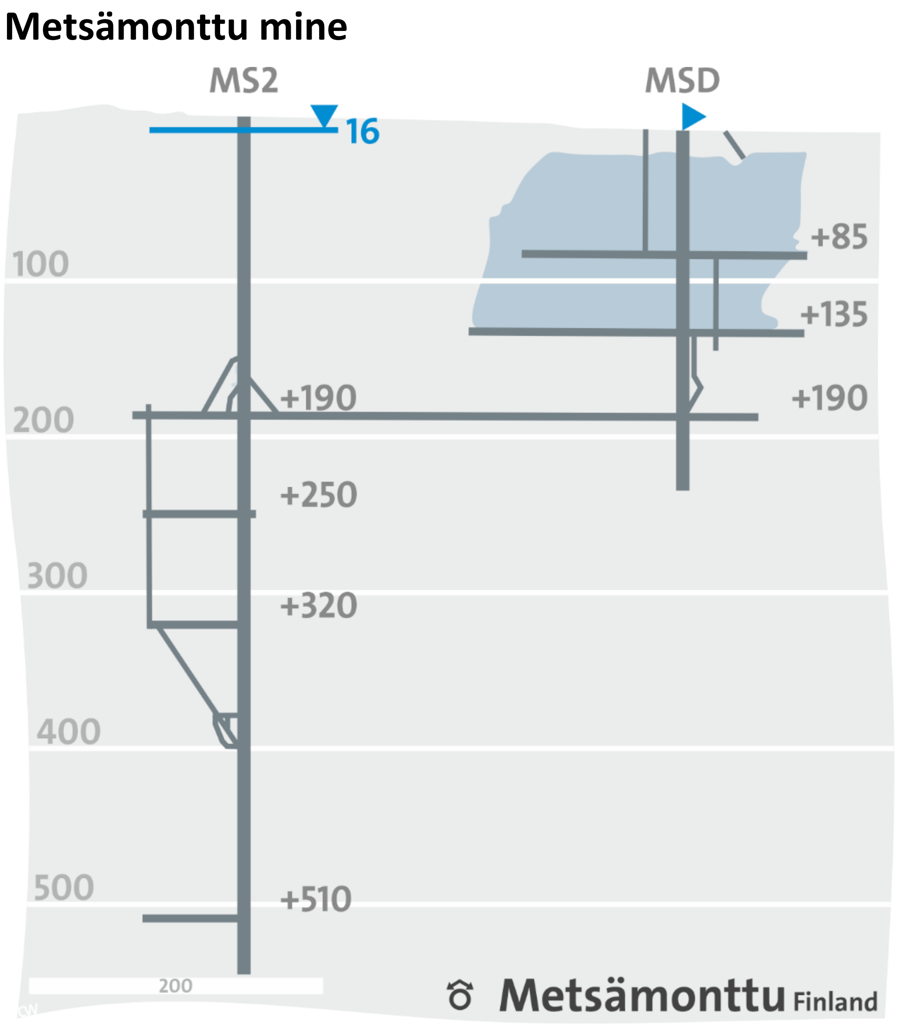

Figure S 44: Cross section of the polymetallic VMS mine Metsämonttu in Finland.

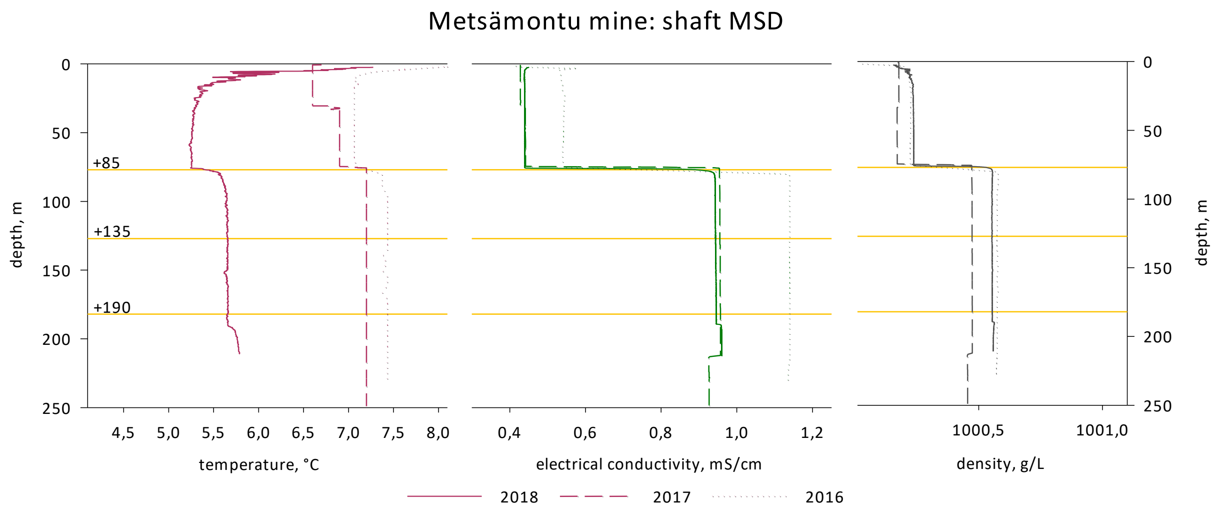

Figure S 45: Temperature profiles (measured), electrical conductivity profiles (measured) and density profiles (calculated with UNESCO equation) of the flooded MSD shaft at the polymetallic VMS mine Metsämonttu in Finland.

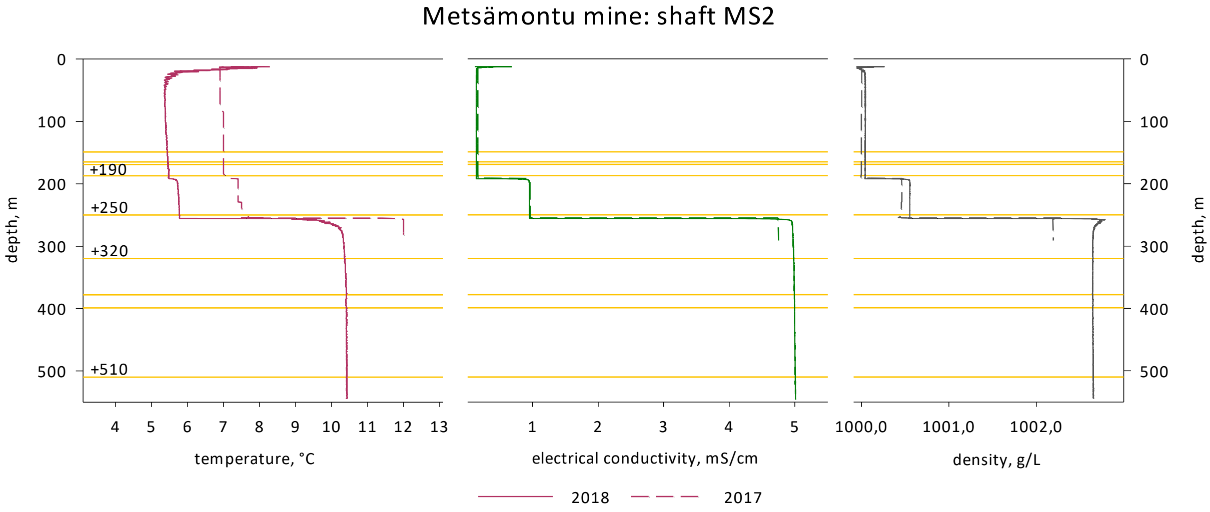

Figure S 46: Temperature profiles (measured), electrical conductivity profiles (measured) and density profiles (calculated with UNESCO equation) of the flooded MS2 shaft at the polymetallic VMS mine Metsämonttu in Finland.

Aijala mine

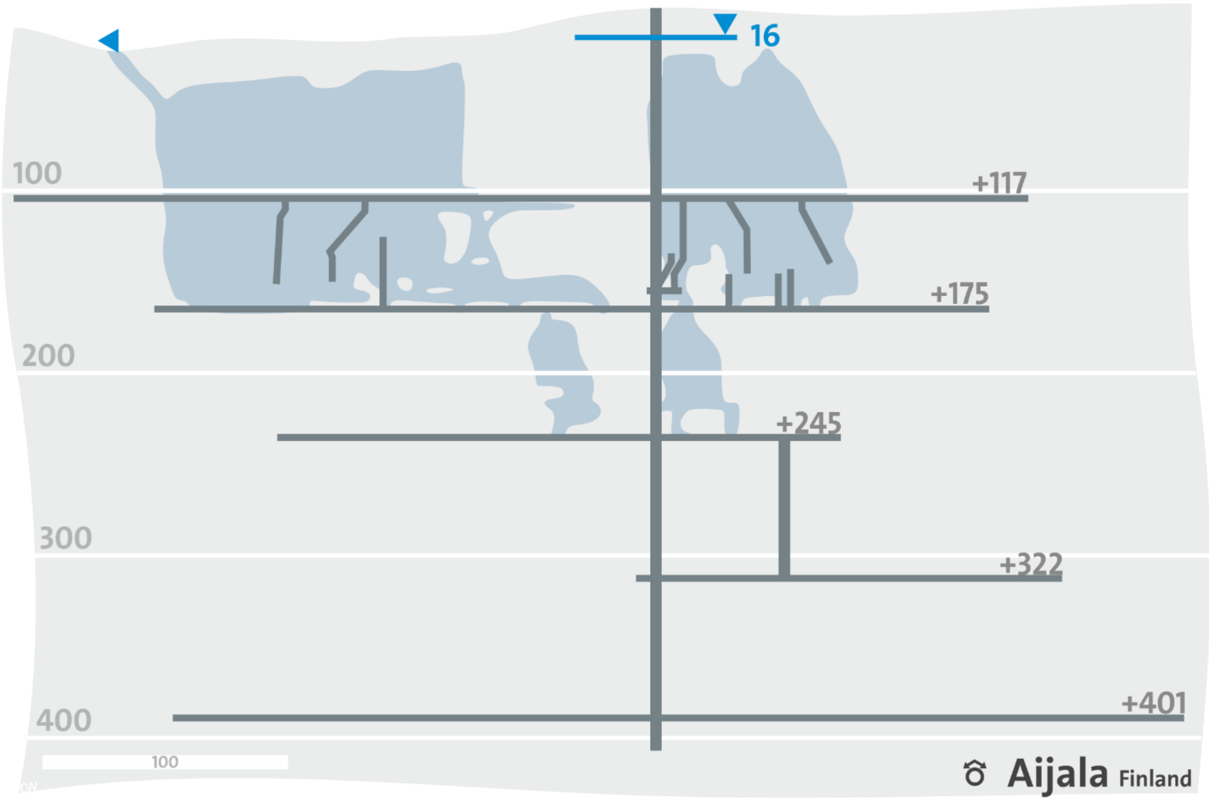

Figure S 47: Cross section of the polymetallic Aijala mine in Finland

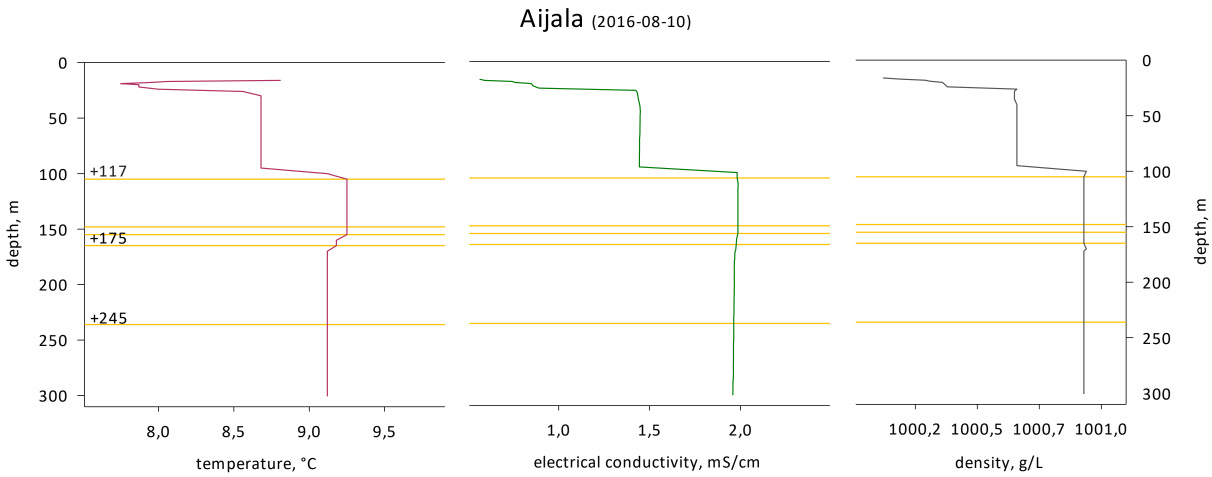

Figure S 48: Temperature profile (measured), electrical conductivity profile (measured) and density profile (calculated with UNESCO equation) of the flooded Aijala mine main shaft in Finland.

Georgi Unterbau silver-copper mine

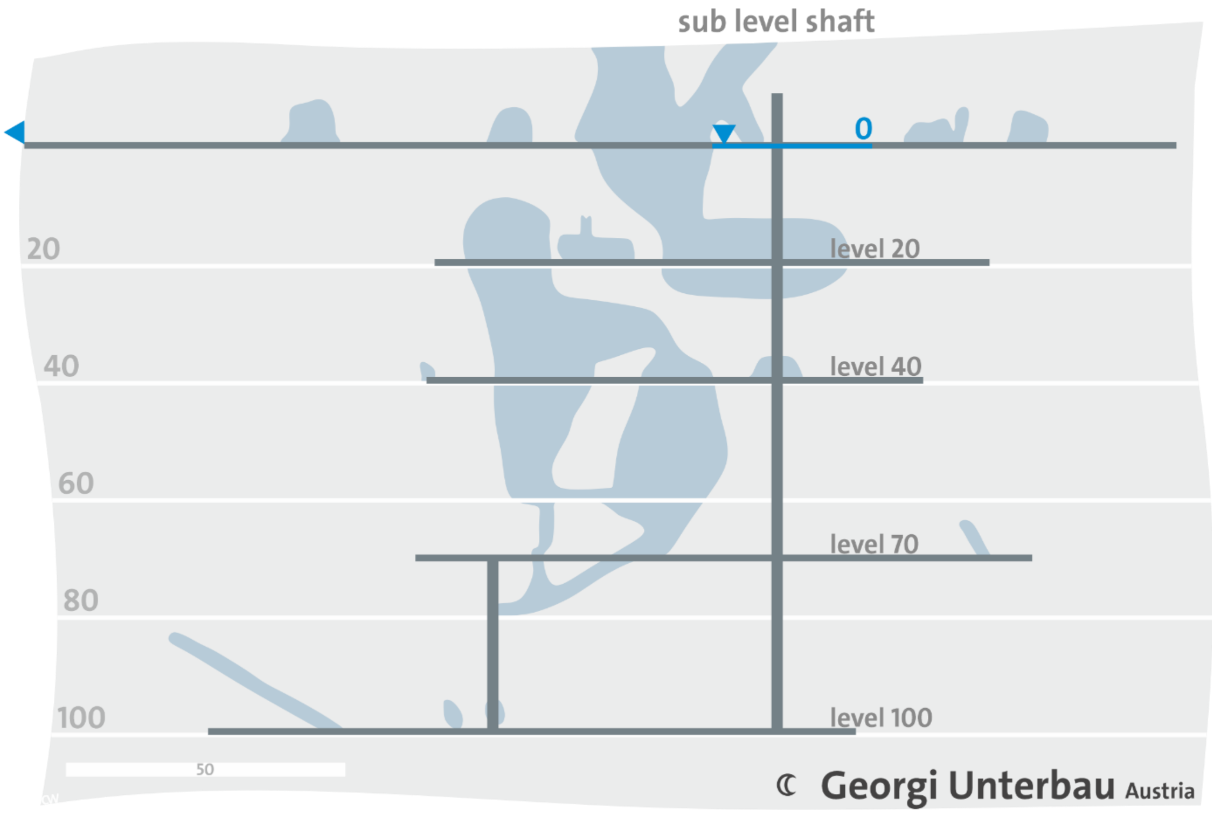

Figure S 49: Cross section of the Georgi Unterbau silver-copper mine in Austria.

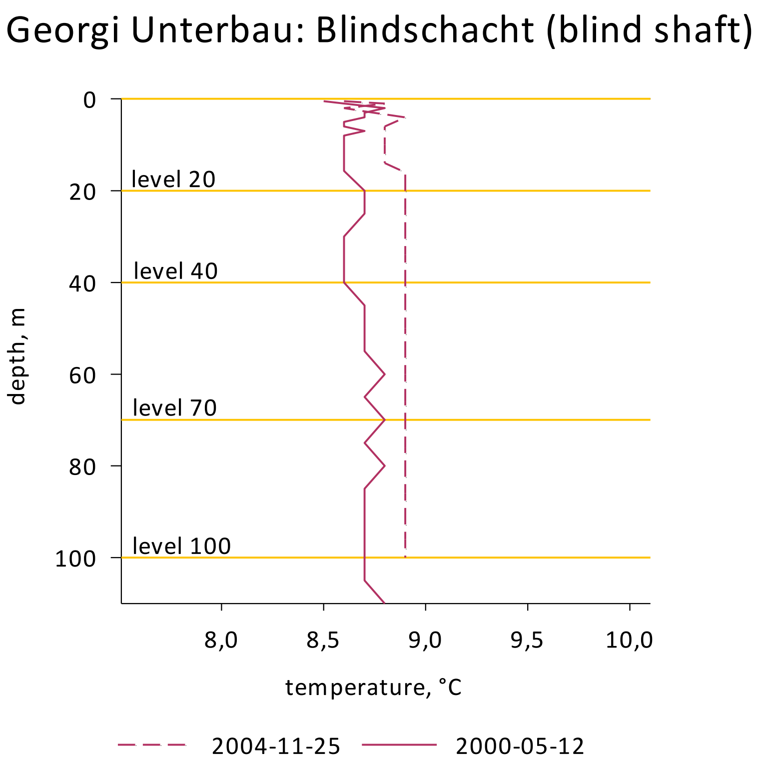

Figure S 50: Temperature profiles (measured) of the flooded Blindschacht at the Georgi Unterbau mine in Austria.

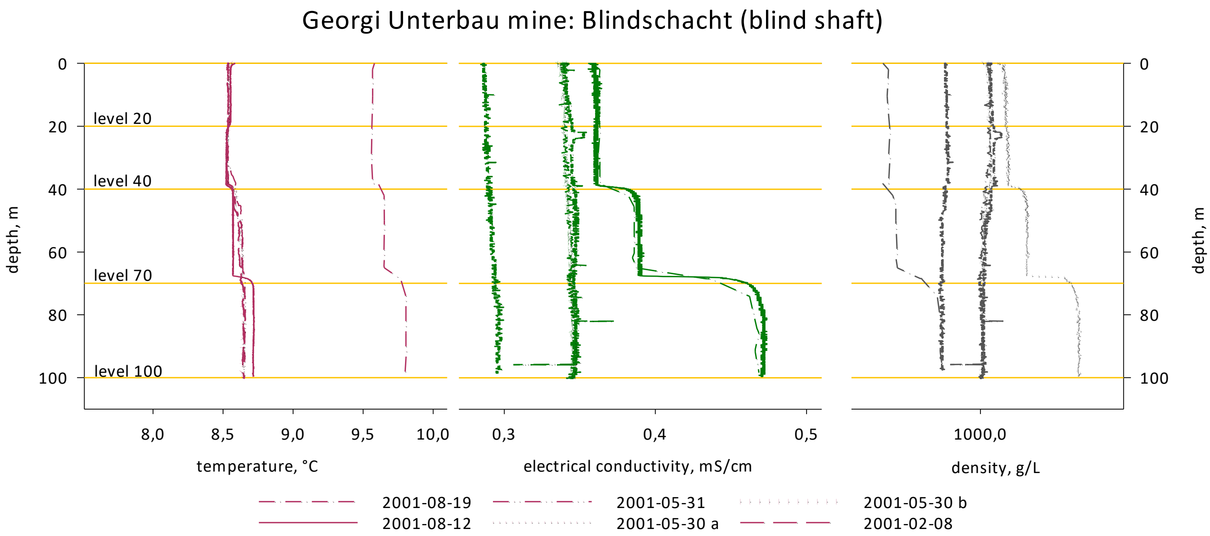

Figure S 51: Temperature profile (measured), electrical conductivity profile (measured) and density profile (calculated with UNESCO equation) of the flooded Blindschacht at the Georgi Unterbau mine in Austria.

Groverake fluorspar mine

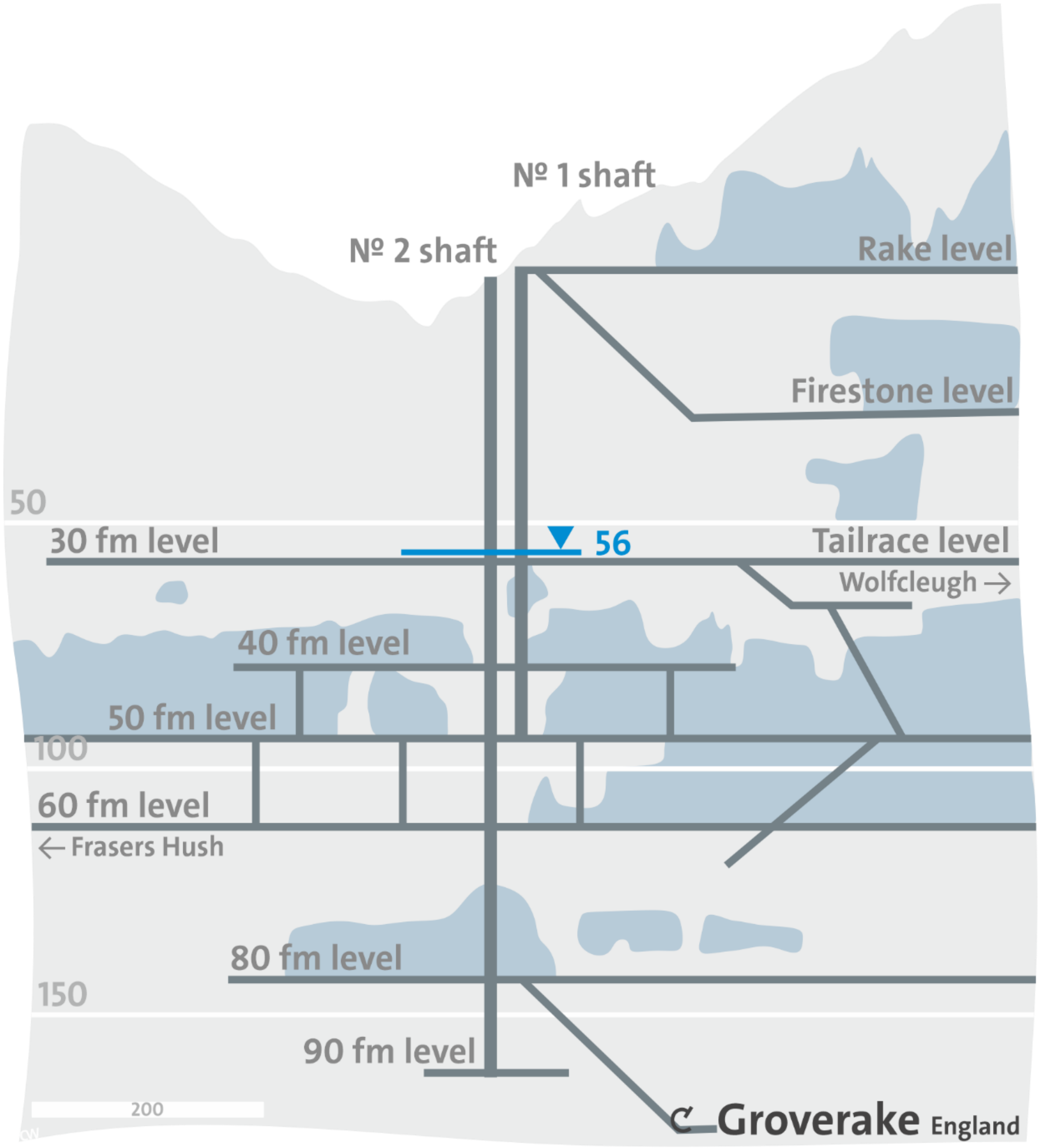

Figure S 52: Cross section of the Groverake fluorspar mine in Great Britain.

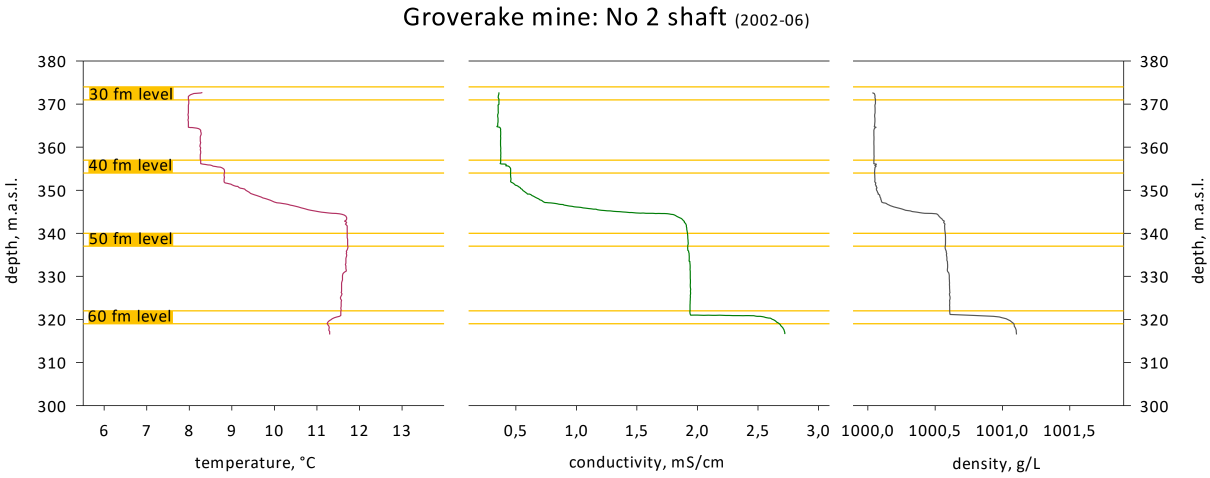

Figure S 53: Temperature profile (measured), electrical conductivity profile (measured) and density profile (calculated with UNESCO equation) of the flooded No 2 shaft at the Groverake fluorspar mine in Great Britain.

Roudný gold mine

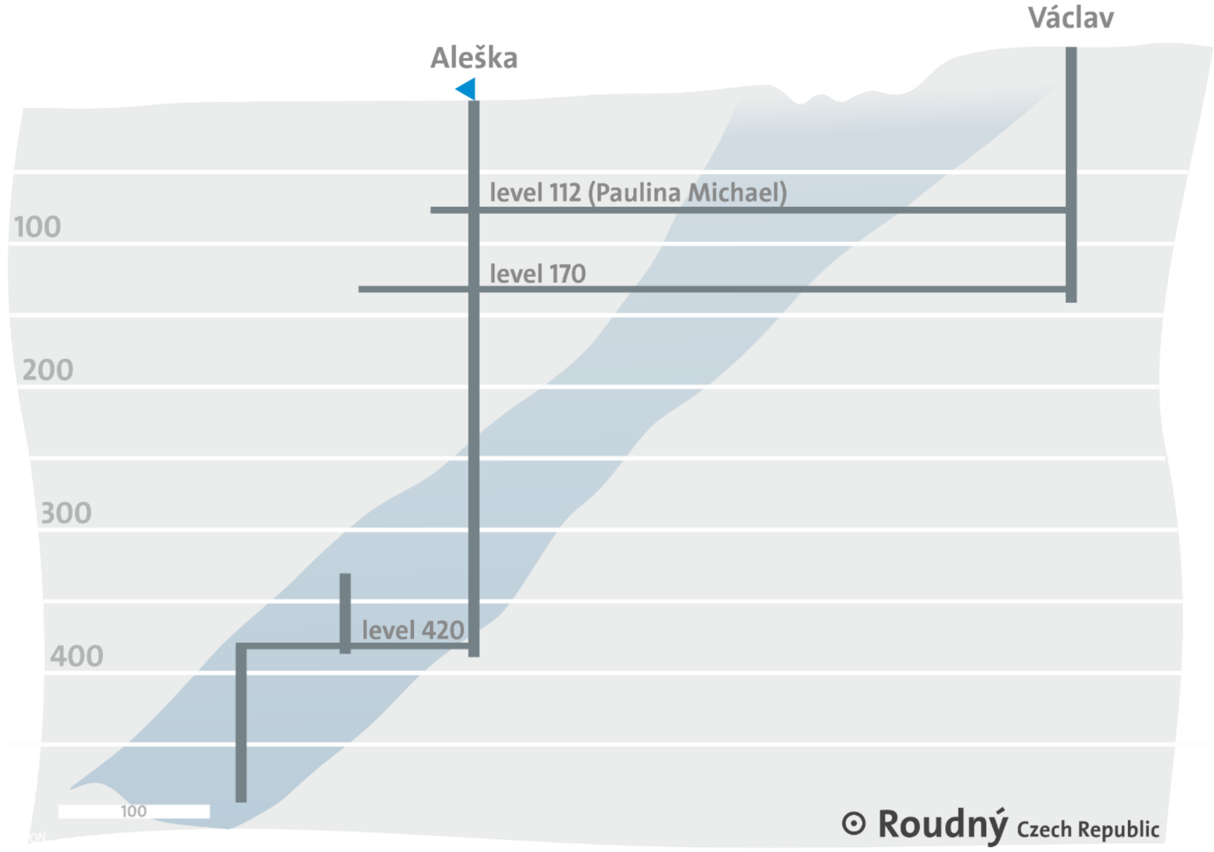

Figure S 54: Cross section of the Roudný gold mine in Czech Republic.

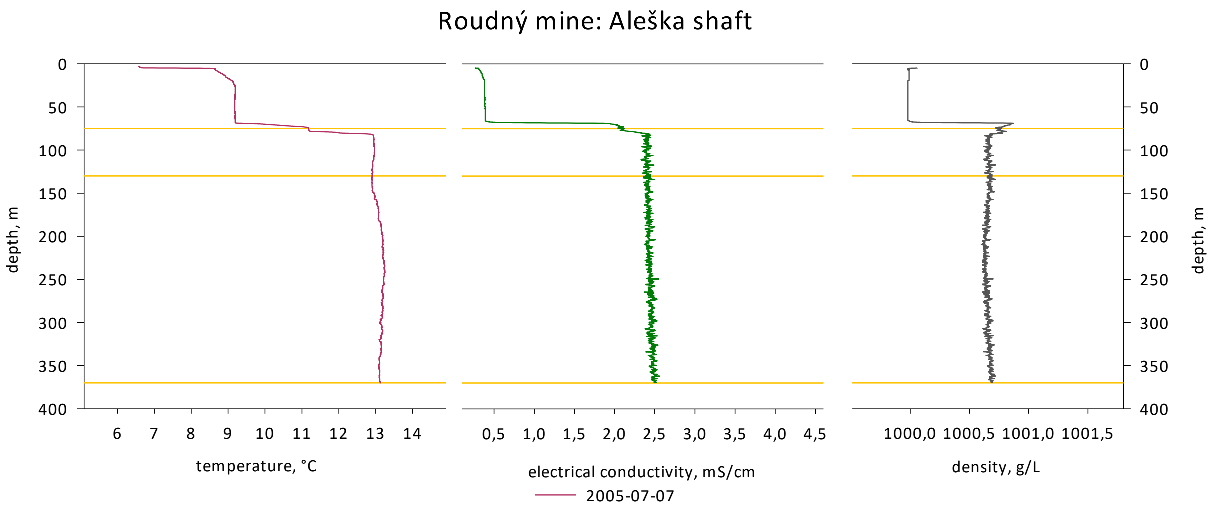

Figure S 55: Temperature profile (measured), electrical conductivity profile (measured) and density profile (calculated with UNESCO equation) of the flooded Aleška shaft at the Roudný gold mine in Czech Republic.

Table: Observations about the topmost (first) intermediate

Table 1: Observations about the topmost (first) intermediate layer at 52 profiles (with two or three water bodies). Horden S40 South Shaft excluded as no cross section available. Shaft profiles in alphabetical order.

mine, shaft name, date of measurement	comment
Aijala (2016)	1st intermediate layer at 1st connected level, convection loop possible
Georgi Unterbau, Blindschacht (2001)	1st intermediate layer at 2nd connected level, 2nd intermediate layer with greater differences of electrical conductivity between the water bodies, 2nd intermediate layer at level 70 where convection loop possible
Grube Georg, Georg Schacht 2 (2006)	intermediate layer and connected level not at the same depth, but probably wrong depth of profile or levels (in that case it can be assumed that 1st intermediate layer at 3rd connected level, convection loop possible)
Grube Georg, Georg Schacht 2 (2008)	intermediate layer and connected level not at the same depth, but probably wrong depth of profile or levels (in that case it can be assumed that 1st intermediate layer at 3rd connected level, convection loop possible)
Grube Georg, Georg Schacht 2 (2009-05)	intermediate layer and connected level not at the same depth, but probably wrong depth of profile or levels (in that case it can be assumed that 1st intermediate layer at 1st connected level), extreme change of depth 1st intermediate layer within 1 year
Grube Georg, Georg Schacht 2 (2009-07)	intermediate layer and connected level not at the same depth, but probably wrong depth of profile or levels (in that case it can be assumed that 1st intermediate layer at 1st connected level), extreme change of depth 1st intermediate layer within 1 year
Grube Merkur, Weidtmann-Schacht	1st intermediate layer at deeper connected level (approx. level 8 in 340 m depth), convection loop possible
Hancock Mine, Shaft 2 (2017?)	1st intermediate layer perhaps at 2nd connected level, depths level with depth profile not clear
Horden, S40 South Shaft (2000)	no statement possible (no cross section available)
Horden, S40 South Shaft (2004)	no statement possible (no cross section available)
Horden, S40 South Shaft (pumping 2000)	no statement possible (no cross section available)
Meggen, Sicilia Schacht (1998-03)	1st intermediate layer at 2nd connected level, convection loop possible
Meggen, Sicilia Schacht (1998-09)	1st intermediate layer at 1st connected level, convection loop possible
Metsämontu, MS2 (2017)	1st intermediate layer at 1st connected level
Metsämontu, MS2 (2018)	1st intermediate layer at 1st connected level, connection to other shaft, 2nd intermediate layer with greater temperature and electrical conductivity differences between the water bodies and at level where convection loop possible
Metsämontu, MSD (2016)	1st intermediate layer at 1st connected level

mine, shaft name, date of measurement	comment
Metsämontu, MSD (2017)	1st intermediate layer not at connected level, 2nd intermediate layer at 1st connected level
Metsämontu, MSD (2018)	1st intermediate layer at 1st connected level
Rosice-Oslavany coal basin, Jindřich II (2004)	1st intermediate layer at deeper connected level (approx. 500 m depth, 4. or 5. level)
Rosice-Oslavany coal basin, Jindřich II (2005)	1st intermediate layer at deeper connected level (approx. 470 m depth, 4. or 5. level)
Rosice-Oslavany coal basin, Jindřich II (2006)	1st intermediate layer at deeper connected level (approx. 480 m depth, 4. or 5. level)
Rosice-Oslavany coal basin, Jindřich II (2007)	1st intermediate layer at deeper connected level (approx. 560 m depth, 4. or 5. level)
Rosice-Oslavany coal basin, Kukla (2004)	probably 1st intermediate layer at 1st connected level (if depths level or depth profile slightly adjusted)
Roudný, Aleška (2005-07)	1st intermediate layer at 1st connected level, convection loop possible
Roudný, Aleška (2005-12)	1st intermediate layer at 1st connected level, convection loop possible
San Vicente, Pozo El Entrego (2008-12-16)	1st intermediate layer at deeper connected level (around level 6, approx. 250 m), but depth profile data not very clear, 1st intermediate layer also possible around 75 m depth (≙ 3rd connected level where convection loop possible)
San Vicente, Pozo El Entrego (2008-12-29)	1st intermediate layer at deeper connected level (around level 6, approx. 250 m),, but depth profile data not very clear, 1st intermediate layer also possible around 75 m depth (≙ 3rd connected level where convection loop possible)
Siège Simon, Simon 5 (2009)	1st intermediate layer at 1st connected level, convection loop possible
Straßberg, Flour Schacht (1992)	1st intermediate layer at 1st connected level
Straßberg, Flour Schacht (1994-12)	1st intermediate layer at 2nd connected level, connection to other shaft
Straßberg, Flour Schacht (1995)	1st intermediate layer at 2nd connected level, connection to other shaft
Straßberg, Flour Schacht (1996-01)	1st intermediate layer at 1st connected level
Straßberg, Flour Schacht (1996-07)	1st intermediate layer at 1st connected level
Straßberg, Flour Schacht (1997)	1st intermediate layer at 1st connected level
Straßberg, Flour Schacht (1998)	1st intermediate layer at 1st connected level
Straßberg, Flour Schacht (1999)	1st intermediate layer at 1st connected level
Straßberg, Flour Schacht (2003)	1st intermediate layer at 2nd connected level, connection to other shaft
Straßberg, Ü539 (1993-05)	1st intermediate layer at 2nd connected level
Straßberg, Ü539 (1993-08)	1st intermediate layer at 2nd connected level
Straßberg, Ü539 (1993-12)	1st intermediate layer at 2nd connected level
Straßberg, Ü539 (1994-07)	1st intermediate layer at 2nd connected level
Straßberg, Ü539 (1994-12)	1st intermediate layer at 2nd connected level
Straßberg, Ü539 (1995)	1st intermediate layer at 2nd connected level
Straßberg, Ü539 (1996)	1st intermediate layer at 2nd connected level
Straßberg, Ü539 (1997)	1st intermediate layer at 2nd connected level
Urgeiriça, St Barbara (2019)	1st intermediate layer at deeper connected level, probably open connection to outflow at shaft P4

mine, shaft name, date of measurement	comment
West Rand, Shaft No 8 (2016)	1st intermediate layer at 2nd connected level (convection loop possible), 2nd intermediate layer 3rd connected level (connection loop possible)
Zeche Glückaufsegen, Glückaufsegen 3 (1997)	probably 1st intermediate layer at 1st connected level (not exact, but measurement inaccuracies can be assumed)
Zeche Glüclaufsege, Glückaufsegen 3 (1989)	1st intermediate layer at 2nd connected level, stratification might have "moved up" between 1989 and 1997
Zeche Hermann, Hermann 1 (1994)	1st intermediate layer at 1st connected level, connection to other shaft, 1st connected level very deep in mine
Zeche Hermann, Hermann 1 (1998)	1st intermediate layer at 1st connected level, connection to other shaft, 1st connected level very deep in mine
Zeche Hermann, Hermann 1 (2003)	1st intermediate layer at 1st connected level, connection to other shaft, 1st connected level very deep in mine
Zeche Hermann, Hermann 1 (2016)	1st intermediate layer at 1st connected level, connection to other shaft, 1st connected level very deep in mine
Zeche Hermann, Hermann 2 (1990)	1st intermediate layer at 1st connected level, connection to other shaft, 1st connected level very deep in mine
Zeche Hermann, Hermann 2 (1994)	1st intermediate layer at 1st connected level, connection to other shaft, 1st connected level very deep in mine
Zeche Hermann, Hermann 2 (1998)	1st intermediate layer at 1st connected level, connection to other shaft, 1st connected level very deep in mine

Glossary

CF (cold freshwater) water body: The CF water body is the uppermost water body in a flooded shaft, which is located above the intermediate layer. Due to its physico-chemical properties (usually lower temperature and lower mineralisation), it differs from the water bodies below the intermediate layer. Alternative terms are upper water body, top layer, near-surface water body, fresh (ground-) water body, clear water zone, shallow sourced water, less mineralized water, meteoric water, freshwater cap or freshwater lens (Henkel and Melchers 2017; Kindermann 1998; Kories et al. 2004; Ladwig et al. 1984; Mugova and Wolkersdorfer 2022; Nuttall and Younger 2003; Rosner 2011; Sanders & Thomas Inc. 1975; Wolkersdorfer 2008).

Convection: Convection occurs when heat is conveyed through the movement of a heated fluid like air or water. In natural convection, this occurs because most fluids tend to expand when heated, becoming less dense and consequently rising due to increased buoyancy. As molecules absorb heat, they speed up, causing expansion and upward movement. Upon cooling, they condense, becoming denser and descending once more, completing a cycle of circulation (Oertel et al. 2017; Rennie and Law 2016).

Convection cells: Convection cells are patterns of fluid motion characterized by circulating currents driven by convection. These cells arise from the interaction between buoyancy forces and gravity, resulting in the upward movement of warmer fluid and the downward movement of cooler fluid, generating circulation patterns. Convection cells can vary in size and shape. Smaller cells in a flooded mine shaft are also called “bales” (American Meteorological Society 2024; Kories et al. 2004).

Convection loops: Convection loops refer to a pattern where convection currents circulate in a closed loop system. These loops often occur in stratified environments or near heat sources, where temperature gradients induce buoyancy-driven flow patterns. In flooded mines the geometry of the loop is defined by the connection between mine shafts, horizontal or inclined galleries and mine voids. The heat source is provided by the geothermal gradient (Bau and Torrance 1981a; b; 1983; Mugova and Wolkersdorfer 2022; Wolkersdorfer 2008).

Density stratification: Density stratification refers to the vertical layering of water masses within a water body based on differences in density, mainly caused by variations in temperature and mineralisation. Denser, or higher mineralised fluid sinks to the bottom, while less dense water rises to the surface, creating horizontal boundaries or interfaces between the layers. This stratification results in distinct water bodies with different physico-chemical properties. Density stratification can occur in natural lakes, pit lakes, seas or oceans, boreholes but also in flooded underground mines (Berthold 2009; Blanc and Anschutz 1995; Boehrer and Schultze 2008; Findenegg 1933; Geller et al. 2013; Mugova and Wolkersdorfer 2022).

Thermal stratification: Thermal stratification refers to the vertical layering of water in a lake, reservoir, or other water body based on temperature differences. In a thermally stratified water body, distinct layers with varying temperatures form, typically with warmer water near the surface and cooler water at greater depths. This stratification occurs due to differences in the heating and cooling rates of water at different depths, as well as the effects of sunlight, wind, and thermal conductivity. Thermal stratification mostly occurs in natural lakes or pit lakes with up to three different layers (epilimnion, metalimnion, hypolimnion; Boehrer and Schultze 2008).

Double diffusive flow/convection: Double diffusive flow or convection refers to a coupled process in fluid dynamics, particularly relevant in the context of mine water movement, where both heat and salinity transport mechanisms interact simultaneously. It occurs when heat and salinity diffuse at different rates within a fluid medium, where heated water usually diffuse more readily than mineralised (salinity) water. This effects the vertical density gradient in opposite directions (Brandt and Fernando 1995; Huppert and Turner 1981; Radko 2013; Rubin and Atkinson 2001).

Internal waves: Internal waves are wave-like disturbances that propagate within a stratified fluid medium, typically occurring at the interface between layers of different densities. Unlike surface waves, which propagate along the water-air interface, internal waves travel within the water column, are caused by density variations within a fluid and induce vertically sheared motion, causing displacement of water parcels (Lerman et al. 1995; Rubin and Atkinson 2001).

Intermediate layer: An interlayer is a usually thin layer between two homogeneous water bodies and is observed in flooded mine shafts between the cold freshwater and the warm mineralised water body or between different warm mineralised water bodies. The intermediate layer can remain stable and not change its position for decades. Only minor exchange between the water bodies below and above the intermediate layer is caused by molecular diffusion (Czolbe et al. 1992; Mugova and Wolkersdorfer 2022; Rüterkamp 2001).

Laminar flow: Laminar flow is a characteristic fluid motion, observed in both gases and liquids, where the fluid moves smoothly in predictable paths. It maintains constant velocity, pressure, and other flow properties and is commonly observed at low flow rates or in highly viscous fluids, where internal friction dominates and suppresses turbulent fluctuations, resulting in predictable flow behaviour (Chapman 1981; Holland and Bragg 1995).

Level: A level is a horizontal passage or roadway that is excavated at a particular elevation within an underground mine. Levels are typically constructed to provide access to ore bodies, facilitate transportation of materials and equipment, and allow for the movement of miners and machinery throughout the mine workings. These passages are often interconnected with vertical shafts, ramps, or other access points, forming a network of tunnels and galleries within the mine. Levels may vary in size and configuration depending on the specific mining method, geological conditions, and operational requirements of the mine (Burghardt et al. 2017; Herrmann and Bucksch 2013; Thrush and Bureau of Mines 1968).

Mine void: A mine void is an underground or open pit cavity or space created by mining activities, typically through the extraction of minerals, ores, or other geological resources. These voids can vary in size and shape depending on the mining method used and the geological characteristics of the deposit. Mine voids may serve various purposes, including storage of waste materials, accommodation of mining infrastructure, or as pathways for ventilation, drainage, or transportation within the mine workings (Cooper 2018; Glencore 2019; Thrush and Bureau of Mines 1968).

Staircase profile: A staircase profile refers to a distinct pattern observed in vertical temperature and salinity profiles within oceanic or other water bodies. This profile, often termed a thermohaline staircase, is characterized by a series of well-mixed water bodies separated by sharp interfaces with high gradients in temperature and mineralisation. These staircases are primarily a result of double diffusive convection processes and turbulent mixing occurring in water bodies, where variations in temperature and salinity/mineralisation lead to the formation of water bodies with different densities. Staircase profiles may exhibit alternating layers of less dense water overlain denser water, forming a visually distinct pattern resembling a staircase when viewed on depth profiles. When turbulent diffusivity surpasses that of double diffusion, staircases are unable to form (Radko et al. 2014).

Turbulent flow: Turbulent flow is a dynamic form of fluid motion, observed in both gases and liquids, characterized by irregular fluctuations and mixing as well as chaotic patterns. It entails continuous changes in the speed and direction of the fluid at various points and typically occurs at high flow rates or in the presence of obstacles. Turbulent flow arises from the interaction of inertial forces and viscous forces within the fluid, leading to the formation of eddies, vortices, and turbulent structures that enhance mixing and transport of momentum, energy, and substances (Chapman 1981; Holland and Bragg 1995).

UNESCO density equation: The UNESCO equation refers to the 1978 agreement among oceanographers to use conductivity as the universal method for estimating the salinity of seawater. It improved accuracy by tracking all ions present in seawater, rather than focusing on chloride alone. UNESCO formally approved this method and included the 1978 Practical Salinity Scale in their 1980 equations for calculating seawater density, known as EOS-80 (Fofonoff and Millard Jr 1983; IOC SCOR and IAPSO 2011).

References for Glossary

American Meteorological Society (2024) Glossary of Meteorology "convection cell". https://glossary.ametsoc.org/wiki/Convection_cell Accessed 28th March 2024

Bau HH, Torrance KE (1981a) On the stability and flow reversal of an asymmetrically heated open convection loop. J Fluid Mech 109:417-433 doi:10.1017/S0022112081001146.

Bau HH, Torrance KE (1981b) Transient and Steady behavior of an open, symmetrically-heated, free convection loop. Int J Heat Mass Transfer 24(4):597-609 doi:10.1016/0017-9310(81)90004-1.

Bau HH, Torrance KE (1983) On the effects of viscous dissipation and pressure work in free convection loops. Int J Heat Mass Transfer 26(5):727-734 doi:10.1016/0017-9310(83)90023-6.

Berthold S (2009) Geophysikalischer Nachweis freier Konvektion in Grundwassermessstellen und Bohrungen [Geophysical determination of free convection in groundwater monitoring wells and boreholes], vol 39. DGFZ, Dresden

Blanc G, Anschutz P (1995) New stratification in the hydrothermal brine system of the Atlantis II Deep, Red Sea. Geology 23(6):543-546 doi:10.1130/0091-7613(1995)023<0543:NSITHB>2.3.CO;2.

Boehrer B, Schultze M (2008) Stratification of lakes. Rev Geophys 46(2) doi:10.1029/2006rg000210.

Brandt A, Fernando HJS (1995) Double-Diffusive Convection, vol 94. American Geophysical Union, Washington

Burghardt D, Coldewey WG, Melchers C, Meßer J, Paul M, Walter T, Wesche D, Westermann S, Wieber G, Wisotzky F, Wolkersdorfer C (2017) Glossar Bergmännische Wasserwirtschaft. Fachsektion Hydrogeologie in der DGGV, Neustadt/Wstr.

Chapman RE (1981) Geology and Water – An introduction to fluid mechanics for geologists, vol 1. Nijhoff Junk, The Hague

Cooper AH (2018) Voids. In: Bobrowsky PT, Marker B (eds) Encyclopedia of Engineering Geology. Springer International Publishing, Cham, p 929-935

Czolbe P, Kretzschmar H-J, Klafki M, Heidenreich H (1992) Strömungszellen im gefluteten Salzschacht [Flow cells in the flooded shaft of a salt mine]. N Bergbautechnik 22(6):213-218.

Findenegg I (1933) Alpenseen ohne Vollzirkulation [Alpine lakes without complete circulation]. Rev Gesamten Hydrobiol 28(3-4):295– 311 doi:10.1002/iroh.19330280309.

Fofonoff NP, Millard Jr RC (1983) Algorithms for computation of fundamental properties of seawater. UNESCO Tech Pap Mar Sci 44:53.

Geller W, Schultze M, Kleinmann R, Wolkersdorfer C (2013) Acidic Pit Lakes – The Legacy of Coal and Metal Surface Mines. Springer, Heidelberg

Glencore (2019) Fact Sheet Final Voids. https://www.glencore.com.au/dam/jcr:ad943824-162a-4e78-91b4-51ca589cb072/2019-final-voids-fact-sheet.pdf Accessed 2nd April 2024

Henkel L, Melchers C (2017) Hydrochemical and isotopegeochemical evaluation of density stratification in mine water bodies of the Ruhr coalfield. In: Wolkersdorfer C, Sartz L, Sillanpää M, Häkkinen A (eds) IMWA 2017 – Mine Water & Circular Economy. LUT Scientific and Expertise Publications, vol 1. Lappeenranta University of Technology Lappeenranta, p 430-436

Herrmann H, Bucksch H (2013) Wörterbuch Geotechnik/Dictionary Geotechnical Engineering – Deutsch-Englisch/German-English, 2nd edn. Springer, Heidelberg

Holland FA, Bragg R (1995) Fluid flow for chemical engineers, 2nd edn. Butterworth-Heinemann, Oxford

Huppert HE, Turner JS (1981) Double-diffusive convection. J Fluid Mech 106:299-329.

IOC SCOR and IAPSO (2011) The International Thermodynamic Equation of Seawater – 2010: A Summary for Policy Makers OC Brochures Series.

Kindermann L (1998) Kontrolle geochemischer Parameter beim Wiedereinbau von Reststoffen in ein stillgelegtes Bergwerk [Control of geochemical parameters during the redeposit of residual materials in a decommissioned mine]. Wiss Mitt Inst Geol 7:196-201.

Kories H, Rüterkamp P, Sippel M Field and numerical studies of water stratification in flooded shafts. In: Jarvis AP, Dudgeon BA, Younger PL (eds) International Mine Water Association Symposium 2004, Newcastle upon Tyne, 2004. vol 1. University of Newcastle, 149-159 p

Ladwig KJ, Erickson PM, Kleinmann RLP, Posluszny ET (1984) Stratification in Water Quality in Inundated Anthracite Mines, Eastern Pennsylvania. Bur Mines Rep Invest 8837:1-35.

Lerman A, Imboden DM, Gat J (1995) Physics and chemistry of lakes. Springer, Berlin

Mugova E, Wolkersdorfer C (2022) Density Stratification and Double-Diffusive Convection in Mine Pools of Flooded Underground Mines – A Review. Water Res doi:10.1016/j.watres.2021.118033.

Nuttall CA, Younger PL (2003) Hydrochemical stratification in flooded underground mines: an overlooked pitfall. J Contam Hydrol 69(1-2):101-114 doi:10.1016/S0169-7722(03)00152-9.

Oertel H, Böhle M, Ehrhard P, Etling D, Müller U, Riedel U, Sreenivasan KR (2017) Prandtl – Führer durch die Strömungslehre – Grundlagen und Phänomene, 14 edn. Springer Vieweg, Braunschweig

Radko T (2013) Double-Diffusive Convection. Cambridge University Press, Cambridge

Radko T, Bulters A, Flanagan JD, Campin J-M (2014) Double-Diffusive Recipes. Part I: Large-Scale Dynamics of Thermohaline Staircases. J Phys Oceanogr 44(5):1269-1284.

Rennie R, Law J (2016) Oxford Dictionary of Chemistry, 7th edn. Oxford University Press, Oxford

Rosner P (2011) Der Grubenwasseranstieg im Aachener und Südlimburger Steinkohlenrevier – eine hydrogeologisch-bergbauliche Analyse der Wirkungszusammenhänge [Mine water rebound in the Aachen and South Limburg coalfields – a hydrogeological-mining analysis of the causal relationships]. PhD Thesis, Rheinisch-Westfälischen Technischen Hochschule Aachen

Rubin H, Atkinson JF (2001) Environmental fluid mechanics. Marcel Dekker, New York

Rüterkamp P (2001) Bildung von Dichteschichtungen in Grubenwässern [Development of density stratification in mine water]. Glückauf Forschungsh 62(2):40-44.

Sanders & Thomas Inc. (1975) Mahanoy Creek Mine Drainage Pollution Abatment Project – Operation Scarlift. Pottstown, Pennsylvania

Thrush PW, Bureau of Mines (1968) A dictionary of mining, mineral, and related terms. U.S. Dept. of the Interior, Washington

Wolkersdorfer C (2008) Water Management at Abandoned Flooded Underground Mines – Fundamentals, Tracer Tests, Modelling, Water Treatment. Springer, Heidelberg